The aminopyridine-3,5-dicarbonitrile core for the design of new non-nucleoside-like agonists of the human adenosine A2Breceptor

The aminopyridine-3,5-dicarbonitrile core for the design of new non-nucleoside-like agonists of the human adenosine A_{2B} receptor

Marco Betti,[a] Daniela Catarzi,[a*] Flavia Varano,[a] Matteo Falsini,[a] Katia Varani,[b] Fabrizio Vincenzi,[b] Diego Dal Ben,[c] Catia Lambertucci,[c] Vittoria Colotta[a]

[a]*Dipartimento di Neuroscienze, Psicologia, Area del Farmaco e Salute del Bambino, Sezione di Farmaceutica e Nutraceutica, Università degli Studi di Firenze, Via Ugo Schiff, 6, 50019 Sesto Fiorentino, Italy;* [b]*Dipartimento di Scienze Mediche, Sezione di Farmacologia, Università degli Studi di Ferrara, Via Fossato di Mortara 17-19, 44121 Ferrara, Italy;* [c]*Scuola di Scienze del Farmaco e dei Prodotti della Salute, Università degli Studi di Camerino, Via S. Agostino 1, 62032 Camerino (MC), Italy.*

AUTHOR INFORMATION

Corresponding author *Tel: +39 055 4573722. e-mail: daniela.catarzi@unifi.it

ORCID: Daniela Catarzi 0000-0002-8821-928X

Highlights

- amino-3,5-dicyanopyridines were developed as novel adenosine hA_{2B} receptor agonists
- some compounds showed nanomolar potency and partial or full agonism at the hA_{2B} AR
- molecular modelling studies were made to simulate the binding mode at the hA_{2B} AR

Abstract

A new series of amino-3,5-dicyanopyridines (**3-28**) as analogues of the adenosine hA_{2B} receptor agonist BAY60-6583 (compound **1**) was synthesized. All the compounds that interact with the hA_{2B} adenosine receptor display EC_{50} values in the range 9-350 nM behaving as partial agonists, with the only exception being the 2-{[4-(4-acetamidophenyl)-6-amino-3,5-dicyanopyridin-2-yl]thio}acetamide (**8)** which shows a full agonist profile. Moreover, the 2-[(1H-imidazol-2-yl)methylthio)]-6-amino-4-(4-cyclopropylmethoxy-phenyl)pyridine-3,5-dicarbonitrile (**15)** turns out to be 3-fold more active than **1** although less selective. This result can be considered a real breakthrough due to the currently limited number of non-adenosine hA_{2B} AR agonists reported in literature. To simulate the binding mode of nucleoside and non-nucleoside agonists at the hA_{2B} AR, molecular docking studies were performed at homology models of this AR subtype developed by using two crystal structures of agonist-bound A_{2A} AR as templates. These investigations allowed us to represent a hypothetical binding mode of hA_{2B} receptor agonists belonging to the amino-3,5-dicyanopyridine series and to rationalize the observed SAR.

Key words: G protein-coupled receptors, adenosine A_{2B} receptor agonists, aminopyridine-3,5-dicarbonitriles, ligand-adenosine receptor modelling studies.

ABBREVIATIONS

ABMECA, N^6-(4-aminobenzyl)-*N*-methylcarboxamidoadenosine; Ado, Adenosine; AR, adenosine receptor; CHO, Chinese hamster ovary; DPCPX, 8-cyclopentyl-1,3-dipropylxanthine; HEPES, 4-(2-hydroxyethyl)-1-piperazineethanesulfonic acid; NECA, 5′-(*N*-ethylcarboxamido)adenosine; EL, extracellular loop; MOE, molecular operating environment; RMS, root-mean-square; TM, transmembrane.

Introduction

Adenosine (Ado) is an endogenous purine nucleoside that normally increases under pathological or stressful situations producing its effects through activation of G protein–coupled adenosine receptors (ARs). These latter, classified as A_1, A_{2A}, A_{2B}, and A_3, are typically coupled to adenylate cyclase but other second messenger systems have also been described [1,2]. Over the years, many ligands, agonists and antagonists, have been identified for the A_1, A_{2A}, and A_3 ARs that, in turn, have been extensively characterized [3]. In contrast, the A_{2B} AR subtype is the least known. In fact, while a large number of selective A_{2B} AR antagonists belonging to different chemical classes has been developed [4-10], only a few A_{2B} AR agonists are known so far [11]. As antagonists are characterized by a large structural variability, the agonist profile has been long associated to an Ado-like structure. Starting from the 5′-(*N*-ethylcarboxamido)adenosine (NECA), the first Ado-derived nucleosidic human (h) A_{2B} AR agonist, a slightly more potent hA_{2B} agonist than NECA was identified [12]. Fortunately, progress has been made. In fact, the non-Ado-like 2-{[6-Amino-3,5-dicyano-4-(4-(cyclopropylmethoxy)phenyl)pyridin-2-yl]thio}acetamide (BAY60-6583, compound **1**), a 2-aminopyridine-3,5-dicarbonitrile derivative (Chart 1) discovered by Bayer Healthcare [13,14], is the only available potent and selective hA_{2B} AR agonist reported so far. Its identification has invalidated the conviction that the sugar moiety is essential for agonism at ARs, such that non-nucleoside ligands must therefore behave as antagonists. Thus, compound **1** has been used extensively as a research tool to clarify the pharmacological roles of A_{2B} AR [15-28] sometimes leading to contradictory results [29]. Thus, it could be a very important goal to obtain other potent and selective hA_{2B} AR agonists especially considering the difficulties that have emerged in understanding of the pharmacological properties of A_{2B} AR agonists and the necessity to explain some controversies concerning the A_{2B}AR [29]. In particular, the amino-3,5-dicyanopyridine series, to which compound **1** belongs, has been demonstrated to include partial agonists with a variable maximum agonist effect at the hA_{2B} AR subtype [30]. More recently, two different papers reported the partial agonist profile of **1** [27,31] and also its potential A_{2B} AR biased agonism was hypothesized [29,32].

Chart 1. Lead structures for the development of currently reported amino-3,5-dicyanopyridine-based AR ligands.

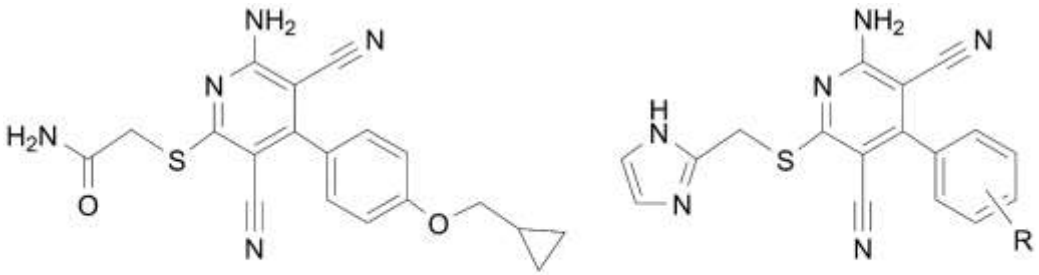

In this scenario, our research group focused attention on the aminopyridine-3,5-dicarbonitrile series to broaden the scarcely known structure-activity relationships (SARs) of this chemical class. In fact, most of the non-Ado-like AR ligands belonging to this series are included in patent documents [12,13,21] while few data are reported in the open literature [30,33,34]. These are, however, sufficient to underline the versatility of the amino-3,5-dicyanopyridine scaffold for producing AR ligands with not only a wide range of affinities but, interestingly, with different degrees of efficacy, ranging from full to partial agonist or neutral antagonist at the different ARs. In particular, certain 2-amino-4-aryl-6-(1H-imidazol-2-yl-methylsulfanyl)-pyridine-3,5-dicarbonitriles belonging to the LUF series [30] (**2**, Chart 1) displayed nanomolar affinity for all the ARs, including the A_{2B} AR subtype on which they showed, in general, also considerable efficacy. Moreover, this class of compounds seems to be more versatile for pharmacological studies showing less species differences than the Ado-like AR agonists [3]. It is worth noting that in addition to compound **1**, that reached preclinical-phase investigation for treating angina pectoris, also other amino-3,5-dicyanopyridine derivatives discovered by Bayer Healthcare have attracted attention for their potential in heart diseases [32, 34]. Thus, taking compound **1** as lead, modifications on the amino-3,5-dicyanopyridine core were performed at both R^1 and R^2 positions (compounds **3-28**, Chart 2).

Chart 2. Modification performed at R^1 and R^2 positions of the 2-amino-4-aryl-6-sulfanyl-3,5-dicyanopyridine scaffold.

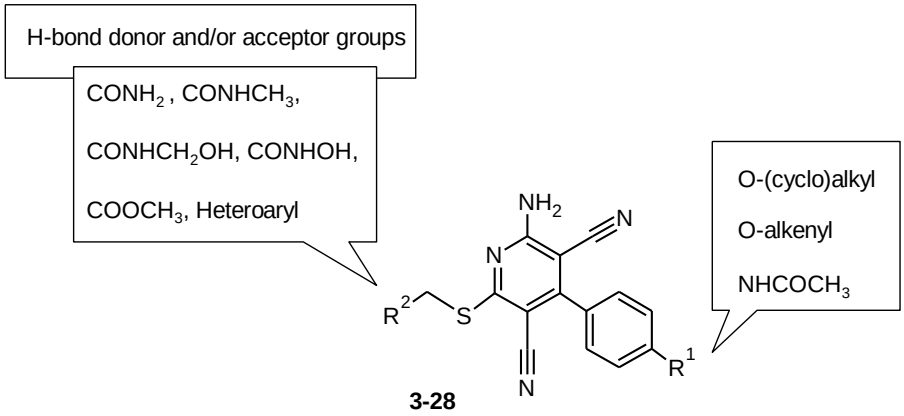

RESULTS AND DISCUSSION

Chemistry

The synthetic pathways which yielded compounds **1**, **3-28**, **52** and the relative intermediates are illustrated in Schemes 1-3. The amino-3,5-dicyanopyridine derivatives **1**, **3-28** [13,21] (Scheme 1) were obtained starting from aldehydes **29-35**, all commercially available with the exception of the 4-(cyclobuthylmethoxy)benzaldehyde **29** [35] which was obtained by reacting 4-hydroxybenzaldehyde with (bromomethyl)cyclobutane in refluxing acetone and in the presence of potassium carbonate. By one-pot cyclization of the suitable aldehyde **29-33**, **35** with malononitrile and thiophenol, the sulfanylphenyl intermediates **37-41**, **43** were obtained. Different cyclization alkaline adjuvants able to work in a phase-transfer system were used, the best being DBU [36]. Moderate to good yields were obtained. Differently, the *para*-acetamido-benzaldehyde **34** was reacted with malononitrile in a straightforward Knoevenagel condensation in the presence of a few drops of piperidine as catalyst to give the intermediate **36** [37]. The latter was reacted with malononitrile in a cyclization reaction involving thiophenol and Et_3N to afford **42** [37].

Scheme 1

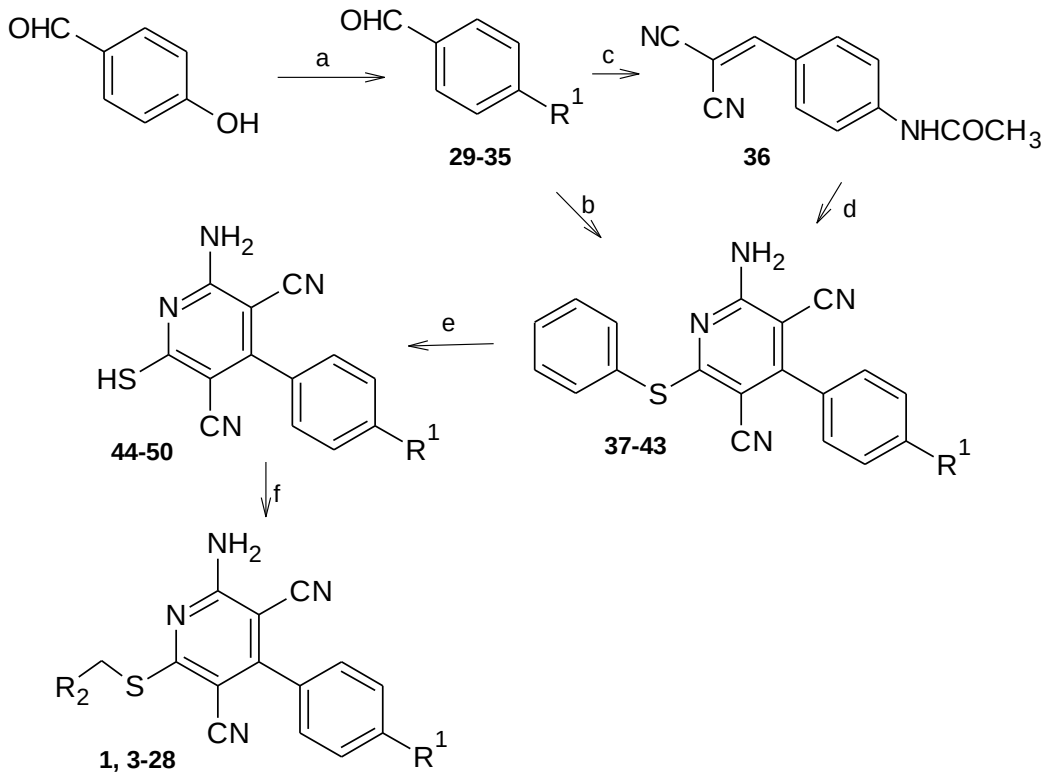

R^1	compound	R^1	compound
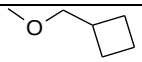	**3, 29, 37, 44**	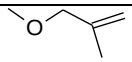	**7, 33, 41, 48**
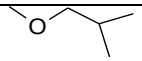	**4, 30, 38, 45**	$NHCOCH_3$	**8, 34, 36, 42, 49**
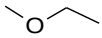	**5, 25-27, 31, 39, 46**	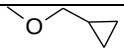	**1, 9-24, 35, 43, 50**
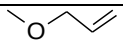	**6, 28, 32, 40, 47**		

Reagents and conditions. a) To yield compound **29**: $BrCH_2C_4H_7$, acetone, anhydrous K_2CO_3, reflux (67%); compounds **30-35** are commercially available; b) malononitrile, thiophenol, DBU, 10% aqueous EtOH, 55 °C (18-37%); c) malononitrile, piperidine, EtOH, 80 °C (63%); d) malononitrile, thiophenol, Et_3N, EtOH, reflux (44%); e) Na_2S, anhydrous DMF, 80 °C; 1M HCl, rt (72-86%); f) R_2CH_2X (X = Cl, Br), $NaHCO_3$, anhydrous DMF, rt (19-80%).

To obtain the free thiols (compounds **44-50** [13,37,38]), the corresponding 6-phenylsulfanyl derivatives **37-43** [37] were treated with sodium sulfide in DMF at 80 °C followed by 1M HCl. The final compounds **3-28** were obtained by reaction of the 6-thiol-derivatives **44-50** with the suitable halides in the presence of sodium hydrogencarbonate. These latter were all commercially available

with the exception of the 2-chloro-N-hydroxyacetamide **51** [39] which was synthesized from ethyl 2-chloroacetate with 50% aqueous solution of hydroxylamine as reported in Scheme 2.

Scheme 2

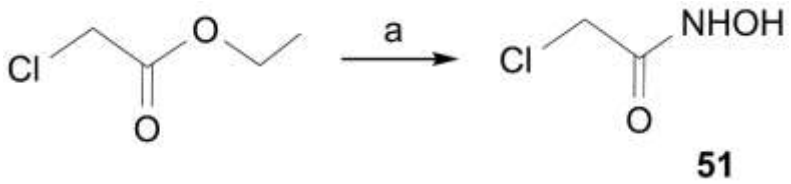

Reagents and conditions. a) 50% aqueous NH_2OH, rt (53%).

Moreover, the hA_{2B} AR agonist **1** [13,21] was cyclized in absolute ethanolic potassium hydroxide to yield the bicyclic compound **52** (Scheme 3). The forced alkaline conditions produced the condensation of the 3-cyano substituent with the active methylene group on the sulfanylacetamide chain [40].

Scheme 3

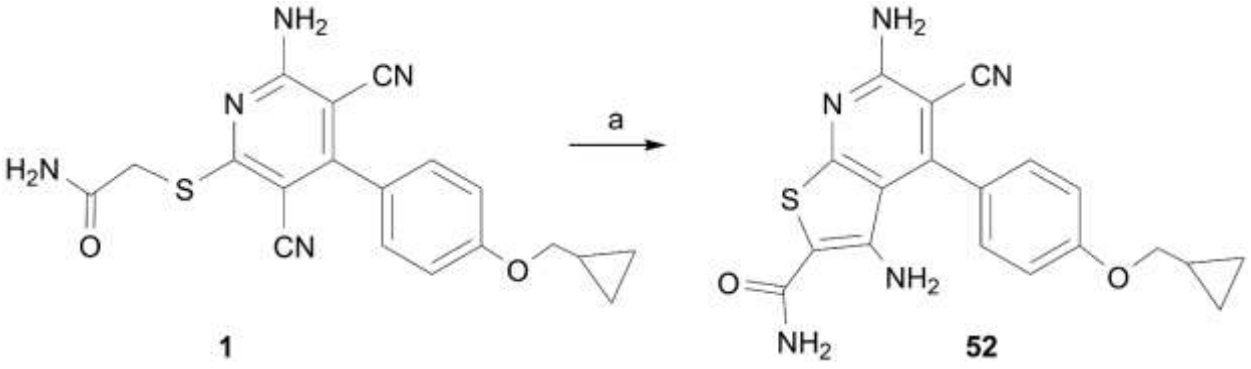

Reagents and conditions. a) KOH, absolute EtOH, reflux (85%).

Pharmacological Assays

The newly synthesized derivatives **3-28**, **52** and the reference compound **1** were studied as hA_{2B} AR agonists by evaluating their stimulatory effect on cAMP production in Chinese Hamster Ovary (CHO) cells, stably expressing the hA_{2B} AR. Some selected compounds (**3, 12, 17, 18, 21-23, 28**) were evaluated also in cAMP production in hA_{2B}CHO cells as hA_{2B} AR antagonists at 1μM concentration in the presence of NECA 100 nM. Moreover, their affinities at hA_1, hA_{2A}, and hA_3 ARs, stably transfected in CHO cells, were measured. All pharmacological data are presented in Table 1.

Table 1. Binding Affinity (K_i) at hA_1, hA_{2A} and hA_3 ARs and potencies (EC_{50}) at hA_{2B} ARs.

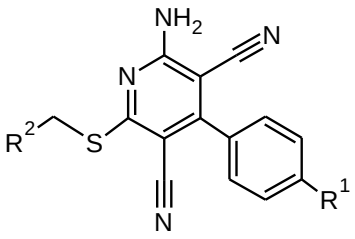

3-28

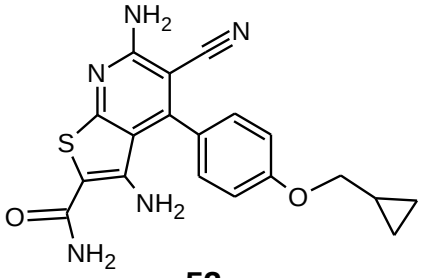

52

			cAMP assays		Binding experiments[a]		
			EC_{50} (nM)[b]	Efficacy,[c] %	K_i (nM) or I%		
	R^1	R^2	hA_{2B}	hA_{2B}	hA_1[d]	hA_{2A}[e]	hA_3[f]
3	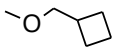	$CONH_2$	-	5%	1%	5%	1%
4	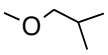	$CONH_2$	-	1%	603± 52	307 ±27	9%
5		$CONH_2$	38±3	66%	345±27	1%	20%
6[g]		$CONH_2$	-	11%	323 ±25	18%	444 ±39
7	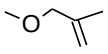	$CONH_2$	-	2%	872±81	31%	4%
8[g]		$CONH_2$	164±12	92%	17%	572±51	742±67
9	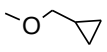	$CONHCH_3$	94±8	63%	14%	1%	3%
10	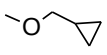	$CONHCH_2OH$	182±14	57%	10%	1%	8%
11	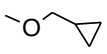	CONHOH	-	20%	536 ± 49	1%	31%

12	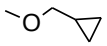	$COOCH_3$	-	1%	23%	1%	1%
13	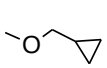	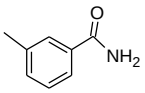	12.7±1.1	69%	83±7	25%	1%
14	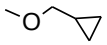	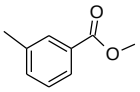	347±31	27%	66±5	1%	4%
15	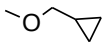		9.5±0.9	70%	235±24	764±72	474±45
16	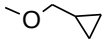		139±11	50%	1%	7%	1%
17	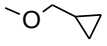		-	7%	483±33	14%	6%
18	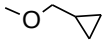	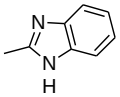	-	12%	21%	6%	1%
19	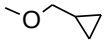		84±6	48%	552±54	2%	6%
20	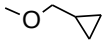		51±4	50%	338±31	1%	1%
21	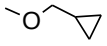		-	25%	3%	1%	1%
22	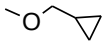	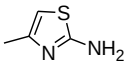	-	17%	140±12	1%	1%
23	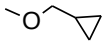		-	1%	12%	1%	1%
24	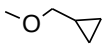		-	1%	67±7	424±37	19%
25		$CONHCH_3$	211 ±17	48%	104 ±8	8%	834 ±74
26			11.7±1.2	62%	8.2±0.7	221±19	85±6
27			332 ±28	34%	21 ±2	4%	18%
28			-	7%	44 ±4	8%	13%
52	-	-	-	1%	19%	3%	13%
1[g,h]	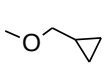	$CONH_2$	31±3	100%	31%	2%	8%

[a] K_i values are means ± SEM of four separate assays each performed in triplicate. Percentage of inhibition (I%) is determined at 1μM concentration of the tested compounds.

[b] EC_{50} values are means ± SEM of four separate assays each performed in triplicate.

[c] Efficacy of the tested compound at 1μM concentration, in comparison with NECA (1μM = 100%).

[d] Displacement of specific [^{3}H]DPCPX competition binding to hA_1CHO cells.

[e] Displacement of specific [^{3}H]ZM241385 competition binding to hA_{2A}CHO cells.
[f] Displacement of specific [^{125}I]AB-MECA competition binding to hA_3CHO cells.
[g] Reference [13].
[h] Reference [21].

Structure-activity relationships

The pharmacological data for the newly synthesized amino-3,5-dicyanopyridine derivatives **3-28** are reported in Table 1 together with those of the reference compound **1** [13,21]. Most of the compounds have generally low to null hA_{2A} and hA_3 AR affinity while the binding at the hA_1 AR subtype depends strictly on both R^1 and R^2 substituents. All the derivatives that interact with the hA_{2B} AR (**5, 8-10, 13-16, 19, 20, 25-27**) display EC_{50} values from 9.5 to 347 nM behaving as partial agonists, with the only exception being compound **8** [13] which shows a full agonist profile. Moreover, derivative **15** that merges the typical R^1 and R^2 substituents of compound **1** and series **2**, respectively (Chart 1), turns out to be the most potent hA_{2B} receptor agonist among this series (EC_{50} = 9.5 nM) and is also endowed with good selectivity versus the other ARs (25-fold vs hA_1 AR, 80-fold vs hA_{2A} AR, and 50-fold vs hA_3 AR). Some compounds (**3, 12, 17, 18, 21-23** and **28**), selected among those that had no activity at the hA_{2B} AR, were evaluated also as hA_{2B} AR antagonists revealing the inability to inhibit NECA-stimulated cAMP levels.

First, to explore how slight modifications of the *para*-cyclopropylmethyloxy group of the lead compound **1** could influence hA_{2B} AR activity and selectivity, 2-sulfanylacetamido-derivatives **3-7** bearing different cycloalkyl- or cycloalkenyl-methyloxy substituents at R^1 position were synthesized. These compounds totally lose hA_{2B} AR activity except for the *para*-ethoxy-substituted derivative **5** which is as potent as **1**. In contrast, the 4-(*para*-acetamidophenyl)-substituted derivative **8** is endowed with good activity at the hA_{2B} AR despite a low selectivity versus hA_{2A} and hA_3 AR subtypes. The latter is the only amino-3,5-dicyanopyridine in the whole series having a full agonist profile at the hA_{2B} AR. The *para*-acetamido substituent, in addition to possessing an oxygen atom as H-bond acceptor, also contains the NH donor group that could have some influence in determining the pharmacological profile of this derivative as observed for series **2** [51,52]. When position R^2 was

modified by introducing carboxamido bioisosteres (compounds **9-14**), best results were obtained in terms of hA_{2B} AR activity and selectivity. In fact, the N-methylacetamido compound **9** and its analogous N-hydroxymethylacetamido **10** are active at the hA_{2B} AR, compound **9** also being the most selective within the herein reported series. In contrast, the hydroxamic acid derivative **11** loses its potency, probably due to the acidity of its R^2 residue which is scarcely tolerated by the hA_{2B} AR. Aryl homologation of the lead **1** yielded compound **13** which is highly potent at the hA_{2B} AR subtype thus confirming how both H-bond acceptor and donor functions at this position are essential for hA_{2B} AR-ligand interaction. Also, the ameliorative π-stacking contribution of the phenyl moiety at R^2 cannot be ignored leading to a great increase of binding affinity at the A_1 subtype.

Starting from the imidazole idea (see series **2**, Chart 1), compound **15** was prepared and it emerged as a very potent hA_{2B} AR agonist being 3-fold more active than the reference agonist **1**. Moreover, it shows good selectivity versus the other AR subtypes and a partial agonist profile. Thus, the imidazolyl moiety at R^2 was replaced with diverse H-bond donor/acceptor-groups containing heterocycles to yield the subset of compounds **16-24**. All derivatives that interact with hA_{2B} AR behave as partial agonist as **15**. First, compound **16** bearing an imidazol-5-yl moiety at R^2 was produced, resulting less active than its isomer **15** at the hA_{2B} AR, but also at the other ARs. Compound **19**, bearing a 3-pyrazolyl group, shows a good hA_{2B} AR affinity that is comparable with that of the 1,2,4-triazol-5-yl derivative **20**. These data, together with the inactivity of compound **23**, confirm again the importance of the presence of H-bond acceptor/donor functions at R^2. Also tetrazolyl-substitution (compound **21)** results as detrimental for hA_{2B} AR activity, probably due to the excessive acidity of the NH tetrazole moiety, as observed for the idroxamic acid derivative **11**.

Furthermore, selecting the best R^1 and R^2 substituents in terms of hA_{2B} AR activity, compounds **25-27** were synthesized bearing the 4-(*para*-ethyloxy) group as a common feature. The potency value of compound **26** confirms the favourable effect exerted by the imidazolyl moiety on hA_{2B} AR interaction making this compound as potent as derivative **15**. In contrast, **26** also shows high hA_1 AR affinity, thus suggesting the cyclopropylmethyloxy substituent as suitable for obtaining potent hA_{2B} AR

agonists endowed with better selectivity versus the other ARs. The same positive effect on hA_1 AR binding is produced by the pyrazolyl group which increases the affinity for this subtype in both derivatives **27** and **28** with respect to the corresponding 2-sulfanylacetamido compounds **5** and **6** [13]. Finally, the bicyclic compound **52**, which was originated by intramolecular cyclization of the parent compound **1**, does not bind any of the ARs thus suggesting that this kind of molecular complication, which makes the structure more rigid, is detrimental for the profitable interaction with hARs and in particular with the A_{2B} AR subtype.

Molecular Modelling Studies

To simulate the binding mode of nucleoside and non-nucleoside agonists at hA_{2B} AR, molecular docking studies were performed on homology models of hA_{2B} AR developed using two crystal structures of agonist-bound hA_{2A} AR [43, 44] as templates (pdb code: 2YDO; 3.0-Å resolution [45] and pdb code: 3QAK; 2.7-Å resolution [46], in complex with Ado and 6-(2,2-diphenylethylamino)-9-[(2*R*,3*R*,4*S*,5*S*)-5-(ethylcarbamoyl)-3,4-dihydroxytetrahydrofuran-2-yl]-*N*-{2-[3-(1-(pyridin-2-yl)piperidin-4-yl)ureido]ethyl}-9*H*-purine-2-carboxamide, also named UK-432097, respectively). The obtained hA_{2B} AR homology models were checked using the Protein Geometry Monitor application within MOE (Molecular Operating Environment 2014.09) [47], with inspection of the structural quality of the protein models (backbone bond lengths, angles and dihedrals, Ramachandran φ-ψ dihedral plots, and quality of side chain rotamer and non-bonded contact). The two hA_{2B} AR structures were then used as target for the docking analysis of the synthesized derivatives, whose structures were optimized using RHF/AM1 semi-empirical calculations (using software package MOPAC implemented in MOE) [48]. The docking studies were performed by using the MOE docking tool and Gold and Autodock software [49-51]. The MOE software analysis was made by selecting the *induced fit* docking and optimization protocol (Schematically, a preliminary docking analysis provides a set of ligand conformations that are energy minimized, including in this step the side chains of the receptor residues in proximity). For each compound, the top-score docking pose at each hA_{2B}

AR model, according to at least two out of three scoring functions, was selected for final ligand-target interaction analysis.

We decided to employ two homology models of the hA_{2B} AR to consider slightly different arrangements of the binding cavities and hence to better explore the conformational variability of the target pocket. Homology models of the hA_{2B} AR built on the same two templates were used for previously reported docking studies with non-nucleoside hAR agonists [51]; the 3QAK A_{2A} AR crystal structure was used as target for docking studies of non-nucleoside agonists of this receptor [52], as well as an X-ray structure of the same protein very similar to the 2YDO structure employed as template in this study (pdb code: 2YDV [45]).

As previously described [51], the binding cavities of the two hA_{2B} AR models are similar, considering both receptor residues orientation and pocket volumes. The differences are due to diverse arrangements of some residues, like a glutamate residue (Glu174, corresponding to Glu169 in hA_{2A} AR) located within extracellular loop (EL) 2 segment and making an H-bond interaction with the N^6-amino group of Ado in the 2YDO crystal structure. This residue is differently oriented in the 3QAK X-ray. For the non-nucleoside agonist binding, the role of this amino acid does not appear to be critical, according to mutagenesis studies performed at A_{2A} AR [52]. The different arrangements of this residue can slightly change the space available at the entrance of the binding cavity, but have a marginal effect on the size and chemical-physical properties of the binding site. This could explain why we observed analogous results by comparing the obtained docking conformations at the two cavities. The Supporting Information section contains a figure showing the two hA_{2B} AR model pockets with the docked compound **15**.

For the sake of clarity, in this section, the position numbering of the substituents on the pyridine nucleus is defined as in compound **15**. Thus, starting from the N1 position, it is assumed that the amino and sulfanyl groups occupy positions 2 and 6, respectively. The simulated binding mode associated to the best score, in the great majority of cases presents the compounds oriented similarly to the one previously described for analogue agonists at hARs (Fig. 1A) [52, 53].

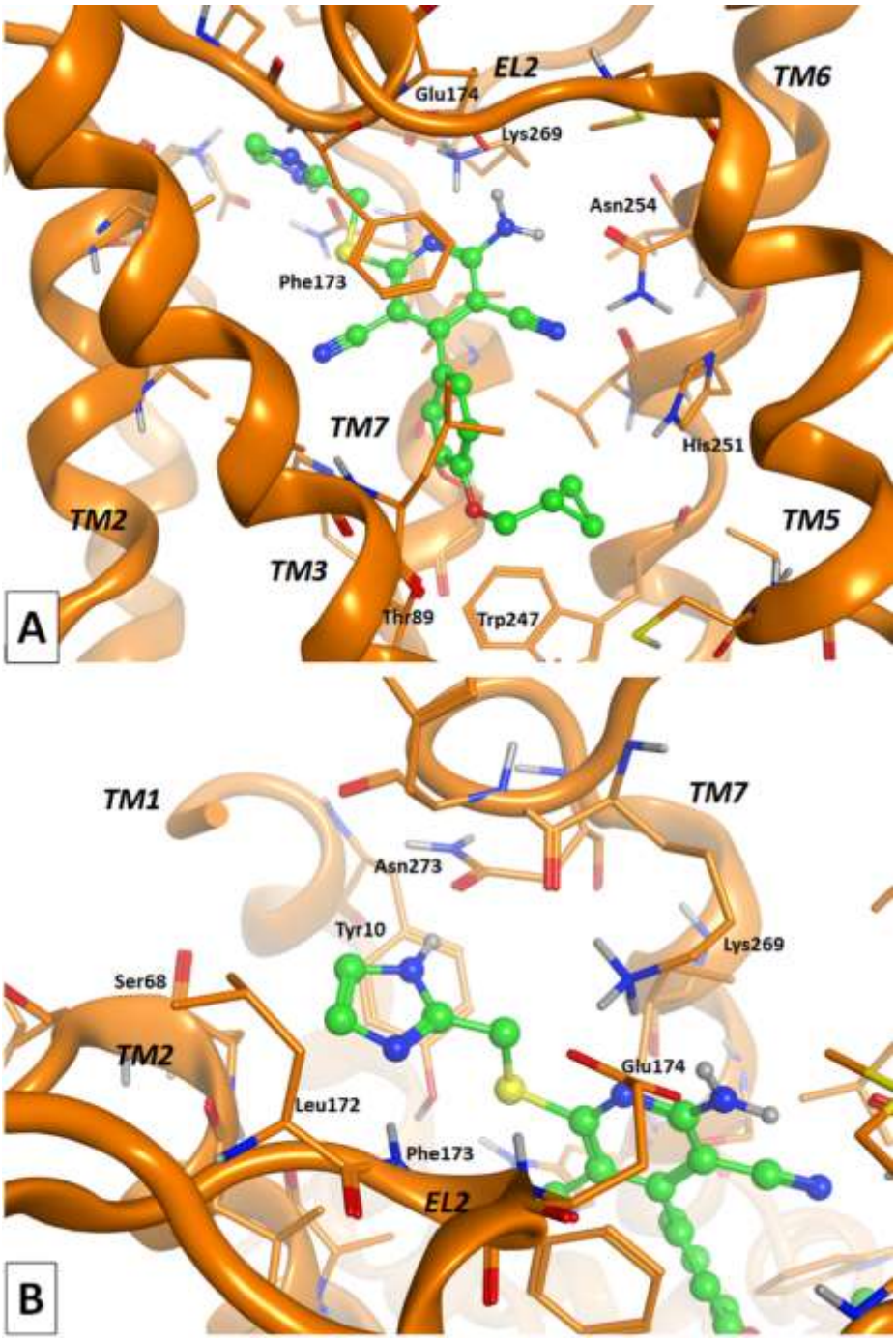

Figure 1. Docking conformation of compound **15** at the hA_{2B} AR receptor model (the 2YDO-based one). Global (A) and top (B) view are displayed. Key residues for ligand-target interaction are indicated.

In detail, the pyridine scaffold is located in the hA_{2B} AR cavity in correspondence to the purine moiety of Ado or UK-432097 observed from hA_{2A} AR templates. The heterocyclic core is stabilized within

the cavity by interaction with Phe173 (EL2) and Ile276$^{7.39}$. Both the 3-cyano and the 2-amino groups make a polar interaction with the amide function of Asn254$^{6.55}$. Considering the 2YDO-based hA_{2B} AR model, the 2-amino substituent gives a H-bond interaction with Glu174, while in the case of the 3QAK-based model such interaction is not present due to a different arrangement of the glutamate. In some cases, the N1 atom makes a polar interaction with Lys269 (EL3). The 5-cyano group on the pyridine core gets in proximity of His280$^{7.43}$ and transmembrane (TM) 2 residues. As previously suggested in analogue studies at the hA_{2A} AR [52], the interaction with these amino acids could be mediated by a bridge water molecule or by a protonated state of His280$^{7.43}$ in which its polar hydrogen could be oriented toward the 3-cyano group. The 6-sulfanyl substituent (Fig. 1B) is located at the entrance of the cavity getting close to residues of TM1, TM2, TM7 domains (Tyr10$^{1.35}$, Ser68$^{2.65}$, and Asn273$^{7.36}$, respectively) and EL2 segment (Leu172 and Phe173). Considering the heterocycle-containing 6-substituents, a series of potential interactions with these residues may be observed (see compounds **15**, **16**, **19** and **20**). Figure 1B shows the imidazol-2-yl moiety appended on the 6-sulfanyl group of **15**. A partial π-stacking interaction is observed with Tyr10$^{1.35}$. The partial reduction of the imidazole ring of **15** (i.e. compound **17**) leads to a fall of hA_{2B} AR activity, possibly due to the loss of this π-stacking interaction. Polar interactions are given by the imidazol-2-yl moiety with the polar hydrogen atom of the backbone amino group of Phe173 and with the carbonyl group of the Asn273$^{7.36}$ side chain. Replacement of the 2-imidazolyl group with a 4-imidazolyl substituent (compound **16**) affords a decrease of activity, probably due to the loss of the interaction with Phe173 polar hydrogen. Other modifications of this ring through the introduction of other nitrogen-containing heterocycles (i.e. **19-21**, **23**) leads to a decrease or a loss of hA_{2B} AR activity. The presence in R^2 of a phenyl ring substituted with an amide or an ester function (compounds **13** and **14**, respectively), still maintains activity at the hA_{2B} AR, confirming the importance of the presence of groups able to provide H-bond interaction at this level. Compounds bringing an amide function within the R^2 substituent are generally endowed with activity at the hA_{2B} AR. This may be interpreted by considering that this functional group mimics the combination of H-bond donor and acceptor functions of the 2-imidazolyl

ring and is able to provide a double polar interaction with Phe173 and Asn273$^{7.36}$ as observed for compound **15**. On the other hand, the activity of the compounds is influenced by the structural and chemical properties of the 4-substituent. In this docking arrangement, this group gets in proximity of Leu86$^{3.33}$, Thr89$^{3.36}$, Trp247$^{6.48}$, His251$^{6.52}$ and, partially, Ser279$^{7.42}$, and His280$^{7.43}$. The volume of the substituent (R^1) at the *para*-position of the 4-phenyl ring appears a critical feature for activity of the compounds, with a cyclopropylmethyloxy function providing the best results at the A_{2B} AR. Docking results show this group located deep in the binding cavity within a narrow hydrophobic sub-pocket that is suitable to accommodate the *para*-cycloalkyl group. This observation helps to interpret the decrease or loss of activity of compounds featuring a *para*-substituent with higher hindrance than the cyclopropylmethyloxy one (i.e. compound **3**). Also, the presence of a smaller *para*-ethyloxy group (compounds **5**, **25-27**) maintains the activity at the hA_{2B} AR although depending on the R_2 substituents as observed in the case of the corresponding *para*-cyclopropylmethyloxyphenyl-substituted derivatives **1**, **9**, **15**, **19**.

An alternative binding mode orients the compounds in a different way with respect to the above described docking conformations, and similarly to the one previously described in the literature at this receptor [50,51,53]. This binding mode is reported and described within the Supporting Information section.

Conclusion

The present study has led to the identification of some potent hA_{2B} AR ligands with a partial agonist profile, several of which are also endowed with good selectivity towards the other AR subtypes. The 2-[(1H-imidazol-2-yl)methylthio)]-6-amino-4-(4-cyclopropylmethoxy-phenyl)pyridine-3,5-dicarbonitrile **15** emerged as the most interesting compound being also 3-fold more active than the lead **1**. This result can be considered a real breakthrough due to the currently limited number of non-Ado-like hA_{2B} AR agonists reported in the literature. The results of the docking studies at two hA_{2B} AR homology models allowed us to interpret the interaction features of the amino-3,5-

dicyanopyridine derivatives at this receptor, also providing useful indications for the design of new hA_{2B} AR ligands belonging to this series.

EXPERIMENTAL PROCEDURES

Chemistry. Analytical silica gel plates (Merck F254), preparative silica gel plates (Merck F254, 2 mm) and silica gel 60 (Merck, 70-230 mesh) were used for analytical and preparative TLC, and for column chromatography, respectively. All melting points were determined on a Gallenkamp melting point apparatus and are uncorrected. Elemental analyses were performed with a Flash E1112 Thermofinnigan elemental analyzer for C, H, N and the results were within ±0.4% of the theoretical values. All final compounds revealed purity not less than 95%. The IR spectra were recorded with a Perkin-Elmer Spectrum RX I spectrometer in Nujol mulls and are expressed in cm^{-1}. NMR spectra were recorded on a Bruker Avance 400 spectrometer (400 MHz for ^{1}H NMR and 100 MHz for ^{13}C NMR). The chemical shifts are reported in δ (ppm) and are relative to the central peak of the residual nondeuterated solvent, which was $CDCl_3$ or $DMSOd_6$. The following abbreviations are used: s = singlet, d = doublet, t = triplet, q = quartet, m = multiplet, br = broad, Ar = aromatic protons, eq = equatorial and ax = axial.

General Procedure for the Synthesis of 6-Substituted 2-Amino-4-aryl-3,5-dicyanopyridine Derivatives 1, **3-21, 23**, **25-28** [13,21] and **2-Substituted 6-Amino-4-aryl-3,5-dicyanopyridines 22**, **24.**

Sodium hydrogen carbonate (2.0 mmol) and the suitable halomethyl-derivative (1.0 mmol) were consequentially added to a solution of the sulfanyl compound **44-50** [13,37,38] (1.0 mmol) in anhydrous DMF (1 mL). The reaction mixture was stirred at rt until the disappearance of the starting material (TLC monitoring). At reaction completion, water was added (25 mL) to precipitate a solid which was collected by filtration and triturated with Et_2O (5 mL). The crude product was purified by

column chromatography (compounds **4**, **7**, **16**, **26**, **27**), preparative TLC (**17**, **28**) or recrystallized (**1**, **3**, **5**, **6**, **8-15**, **18-25**).

*2-{[6-Amino-3,5-dicyano-4-(4-(cyclopropylmethoxy)phenyl)pyridin-2-yl]thio}acetamide **1*** [13,21].

Yield 40%; mp 219-220 °C (MeOH); ^{1}H NMR (DMSO-d_6) 8.00 (br s, 2H, NH_2), 7.45-7.55 (m, 3H, Ar + NH), 7.25 (s, 1H, NH), 7.10 (d, 2H, Ar, J= 8.7 Hz), 3.91 (d, 2H, OCH_2, J= 7.0 Hz), 3.88 (s, 2H, SCH_2), 1.23-1.29 (m, 1H, CH), 0.58-0.62 (m, 2H, CHeq), 0.34-0.38 (m, 2H, CHax). Anal. Calcd for $C_{19}H_{17}N_5O_2S$.

*2-{[6-Amino-3,5-dicyano-4-(4-(cyclobutylmethoxy)phenyl)pyridin-2-yl]thio}acetamide **3***.

Yield 21%; mp 244-246 °C (EtOAc/cyclohexane); ^{1}H NMR (DMSO-d_6) 7.99 (br s, 2H, NH_2), 7.50-7.47 (m, 3H, Ar + NH), 7.49 (d, 2H, Ar, J= 8.6 Hz), 7.26 (s, 1H, NH), 7.10 (d, 2H, Ar, J= 8.6 Hz), 4.04 (d, 2H, OCH_2, J= 6.7 Hz), 3.88 (s, 2H, SCH_2), 2.78- 2.71 (m, 1H, CH), 1.99-1.82 (m, 6H, $3CH_2$); IR 3664, 3361, 3252, 2214, 1635. Anal. Calcd for $C_{20}H_{19}N_5O_2S$.

*2-{[6-Amino-3,5-dicyano-4-(4-isobutoxyphenyl)pyridin-2-yl]thio}acetamide **4***.

Yield 21%; column chromatography, eluting system CH_2Cl_2/MeOH, 9.7:0.3; mp 233-235 °C (EtOH); ^{1}H NMR (DMSO-d_6) 7.99 (br s, 2H, NH_2), 7.49-7.47 (m, 3H, Ar + NH), 7.25 (s, 1H, NH), 7.11 (d, 2H, Ar, J= 8.8 Hz), 3.88 (s, 2H, SCH_2), 3.84 (d, 2H, OCH_2, J= 6.4 Hz), 2.08-2.02 (m, 1H, CH), 1.01 (d, 6H, $2CH_3$, J= 6.8 Hz); IR 3537, 3375, 3196, 2208, 1639. Anal. Calcd for $C_{19}H_{19}N_5O_2S$.

*2-{[6-Amino-3,5-dicyano-4-(4-ethoxyphenyl)pyridin-2-yl]thio}acetamide **5***.

Yield 35%; mp 235-237 °C (EtOH); ^{1}H NMR (DMSO-d_6) 7.98 (br s, 2H, NH_2), 7.50 (s, 1H, NH), 7.48 (d, 2H, Ar, J= 8.8 Hz), 7.23 (s, 1H, NH), 7.10 (d, 2H, Ar, J= 8.8 Hz), 4.12 (q, 2H, OCH_2, J= 7.2 Hz), 3.88 (s, 2H, SCH_2), 1.36 (t, 3H, CH_3, J= 7.2 Hz,); IR 3396, 3180, 2210, 1637. Anal. Calcd for $C_{17}H_{15}N_5O_2S$.

*2-{[4-(4-(Allyloxy)phenyl)-6-amino-3,5-dicyanopyridin-2-yl]thio)}acetamide **6*** [13].

Yield 67%; mp 204-206 °C (EtOH); ^{1}H NMR (DMSO-d_6) 8.00 (s, 2H, NH_2), 7.50 (m, 3H, Ar + NH), 7.26 (s, 1H, NH), 7.14 (d, 2H, Ar, J = 8.7 Hz), 5.98-6.18 (m, 1H, CH), 5.45 (dd, 1H, CH_2, J = 17.3,

1.4 Hz), 5.30 (dd, 1H, CH, J = 10.5, 1.4 Hz), 4.67 (d, 2H, OCH_2, J = 5.1 Hz), 3.89 (s, 2H, SCH_2); IR 3325, 3215, 3184, 2212. Anal. Calcd for $C_{18}H_{15}N_5O_2S$.

*2-{[6-Amino-3,5-dicyano-4-(4-[(2-methylallyl)oxy]phenyl)pyridin-2-yl]thio}acetamide **7**.*

Yield 27%; column chromatography, eluting system EtOAc/cyclohexane/MeOH, 5:5:1); mp 224-226 °C (EtOH); ^{1}H NMR (DMSO-d_6) 7.99 (s, 2H, NH_2), 7.51 (s, 1H, NH), 7.50 (d, 2H, Ar, J= 8.6 Hz), 7.25 (s, 1H, NH), 7.13 (d, 2H, Ar, J= 8.6 Hz), 5.10 (s, 1H, CH), 4.99 (s, 1H, CH), 4.57 (s, 2H, OCH_2), 3.88 (s, 2H, SCH_2), 1.08 (s, 3H, CH_3); IR 3481, 3334, 3234, 2212, 1681. Anal. Calcd for $C_{19}H_{17}N_5O_2S$.

*2-{]4-(4-Acetamidophenyl)-6-amino-3,5-dicyanopyridin-2-yl]thio}acetamide **8*** [13].

Yield 19%; 279-281 °C (MeOH); ^{1}H NMR (DMSO-d_6) 10.2 (br s, 1H, NH), 7.99 (br s, 2H, NH_2), 7.74 (d, 2H, Ar, J= 7.6 Hz), 7.49-7.47 (m, 3H, Ar + NH), 7.24 (s, 1H, NH), 3.89 (s, 2H, SCH_2), 2.09 (s, 3H, CH_3); ^{13}C NMR (DMSO-d_6): 169.38, 169.27, 166.67, 160.10, 158.52, 141.70, 129.72, 128.44, 119.12, 115.82, 93.65, 86.29, 33.78, 24.57; IR 3419, 3367, 2208, 1647. Anal. Calcd for $C_{17}H_{14}N_6O_2S$.

*2-{[6-Amino-3,5-dicyano-4-(4-(cyclopropylmethoxy)phenyl)pyridin-2-yl]thio}-N-methylacetamide **9**.*

Yield 71%; mp 274-276 °C (Acetone); ^{1}H NMR (DMSO-d_6) 8.20-7.90 (bm, 3H, NH_2 + NH), 7.47 (d, 2H, Ar, J = 8.7 Hz), 7.09 (d, 2H, Ar, J = 8.7 Hz), 3.85-3.95 (m, 4H, SCH_2 + OCH_2), 2.62 (d, 3H, CH_3, J = 4.6 Hz), 1.23-1.30 (m, 1H, CH), 0.57-0.61 (m, 2H, CHeq), 0.34-0.38 (m, 2H, CHax); ^{13}C NMR (DMSO-d_6): 167.79, 166.54, 160.76, 160.16, 158.59, 130.64, 126.04, 115.90, 115.00, 93.70, 86.24, 72.75, 33.73, 26.56, 10.53, 3.61. IR 3390, 3323, 3223, 2208. Anal. Calcd for $C_{20}H_{19}N_5O_2S$.

*2-{[6-Amino-3,5-dicyano-4-(4-(cyclopropylmethoxy)phenyl)pyridin-2-yl]thio}-N-(hydroxymethyl)-acetamide **10**.*

Yield 79%; mp 202-204°C (MeOH); ^{1}H NMR (DMSO-d_6) 8.69 (t, 1H, NH, J= 6.3 Hz); 7.8-8.2 (br s, 2H, NH_2), 7.46-7.50 (m, 2H, Ar), 7.08-7.12 (m, 2H, Ar), 5.72 (t, 1H, OH, J = 6.42 Hz), 4.53 (t, 2H, NCH_2O, J= 6.00), 3.90-3.92 (m, 4H, $2CH_2$), 1.22-1.29 (m, 1H, CH), 0.58-0.62 (m, 2H, CHeq), 0.34-0.38 (m, 2H, CHax); IR 3394, 3319, 3224, 2208, 1639. Anal. Calcd for $C_{20}H_{19}N_5O_3S$.

2-{[6-Amino-3,5-dicyano-4-(4-(cyclopropylmethoxy)phenyl)pyridin-2-yl]thio}-N-hydroxyacetamide ***11***.

Yield 60%; mp 176-178 °C (EtOH); ^{1}H NMR (DMSO-d_6) 10.58 (br s, 1H, OH), 9.06 (br s, 1H, NH), 8.01 (br s, 2H, NH_2), 7.48 (d, 2H, Ar, J = 8.6 Hz,), 7.10 (d, 2H, Ar, J = 8.6 Hz), 3.91 (d, 2H, SCH_2, J = 6.9 Hz), 3.81 (s, 2H, OCH_2), 1.27-1.24 (m, 1H, CH), 0.58-0.62 (m, 2H, CHeq), 0.37 – 0.42 (m, 2H, CHax); IR 3649, 3331, 3223, 2208. Anal. Calcd for $C_{19}H_{17}N_5O_3S$.

Methyl 2-{[6-amino-3,5-dicyano-4-(4-(cyclopropylmethoxy)phenyl)pyridin-2-yl]thio}acetate ***12***.

Yield 41%; mp 205-207 °C (EtOH); ^{1}H NMR (DMSO-d_6) 7.9 (br s, 2H, NH_2), 7.48 (d, 2H, ar J= 8.8), 7.1 (d, 2H, ar, J= 8.8), 4.20 (s, 2H, SCH_2), 3.91 (d, 2H, OCH_2, J= 7.0), 3.69 (s, 3H, OCH_3), 1.24-1.28 (m, 1H, CH), 0.58-0.62 (m, 2H, CHeq), 0.35-0.38 (m, 2H, CHax); IR 3446, 3342, 3224, 2210, 1739. Anal. Calcd for $C_{20}H_{18}N_4O_3S$

3-{[(6-Amino-3,5-dicyano-4-[4-(cyclopropylmethoxy)phenyl]pyridin-2-yl)thio]methyl}benzamide ***13***.

Yield 47%; mp 243-245 °C (EtOAc/2-methoxyethanol); ^{1}H NMR (DMSO-d_6) 8.05 (br s, 2H, NH_2), 8.00 (s, 1H, Ar), 7.96 (s, 1H, NH), 7.77 (d, 1H, Ar, J= 7.8 Hz), 7.69 (d, 1H, Ar, J= 7.7 Hz), 7.47-7.38 (m, 4H, 3ar + NH), 7.07 (d, 2H, Ar, J= 8.8 Hz), 4.54 (s, 2H, SCH_2), 3.90 (d, 2H, OCH_2, J= 7.0), 1.23-1.28 (m, 1H, CH), 0.58-0.61 (m, 2H, CHeq), 0.33-0.37 (m, 2H, CHax); IR 3441, 3387, 3356, 3169, 2212, 1635. Anal. Calcd for $C_{25}H_{21}N_5O_2S$.

Methyl 3-{[(6-amino-3,5-dicyano-4-[4-(cyclopropylmethoxy)phenyl]pyridin-2-yl)thio]methyl} benzoate ***14***.

Yield 58%; mp 158-160 °C (MeOH); ^{1}H NMR (DMSO-d_6) 8.10 (s, 1H, ar), 7.90-8.35 (br s, 2H, NH_2), 7.84-7.87 (m, 2H, Ar), 7.44-7.49 (m, 3H, Ar), 7.07 (d, 2H, ar, J= 8.8 Hz), 4.59 (s, 2H, SCH_2), 3.90 (d, 2H, OCH_2 J= 7.04), 3.86 (s, 3H, OCH_3), 1.23-1.27 (m, 1H, CH), 0.58-0.62 (m, 2H, CHeq), 0.34-0.37 (m, 2H, CHax); IR 3396, 3331, 3230, 2210, 1707. Anal. Calcd for $C_{26}H_{22}N_4O_3S$.

2-{[(1H-Imidazol-2-yl)methyl]thio}-6-amino-4-[4-(cyclopropylmethoxy)phenyl]pyridine-3,5-dicarbonitrile ***15***.

Yield 63%; mp 226-228 °C (EtOH); ^{1}H NMR (DMSO-d_6) 11.8 (s, 1H, NH), 8.07 (br s, 2H, NH_2), 7.47 (d, 2H, Ar, J = 8.2 Hz), 7.09 (d, 2H, Ar, J = 8.2 Hz); 6.90 (br s, 2H, CH, Ar), 4.49 (s, 2H, SCH_2), 3.90 (d, 2H, OCH_2, J = 8.0 Hz), 1.23-1.29 (m, 1H, CH), 0.62-0.58 (m, 2H, CHeq), 0.39-0.35 (m, 2H, CHax); ^{13}C NMR (DMSO-d_6): 166.59, 160.74, 160.32, 158.58, 155.20, 143.02, 130.64, 126.03, 115.96, 115.91, 114.98, 93.64, 86.38, 72.75, 27.21, 10.53, 3.62; IR 3430, 3387, 2229. Anal. Calcd for $C_{21}H_{18}N_6OS$.

2-{[(1H-Imidazol-5-yl)methyl]thio}-6-amino-4-[4-(cyclopropylmethoxy)phenyl]pyridine-3,5-dicarbonitrile ***16****.*

Yield 32%; column chromatography, eluting system $CHCl_3$/MeOH, 9:1); mp 186-188 °C (EtOH); ^{1}H NMR (DMSO-d_6) 11.97 (s, 1H, NH), 8.04 (br s, 2H, NH_2), 7.59 (s, 1H, Ar), 7.47 (d, 2H, Ar, J = 8.5 Hz), 7.18 (s, 1H, Ar), 7.08 (d, 2H, Ar J= 8.5 Hz), 4.40 (s, 2H, SCH_2), 3.90 (d, 2H, OCH_2, J= 6.9 Hz), 1.23-1.27 (m, 1H, CH), 0.63- 0.57 (m, 2H, CHeq), 0.34-0.37 (m, 2H, CHax); ^{13}C NMR (DMSO-d_6): 167.24, 160.67, 160.18, 158.49, 130.63, 126.16, 116.02, 114.95, 93.81, 86.05, 72.73, 10.53, 3.60; IR 3318, 3205, 3080, 2212. Anal. Calcd for $C_{21}H_{18}N_6OS$.

2-Amino-4-[4-(cyclopropylmethoxy)phenyl]-6-{[(4,5-dihydro-1H-imidazol-2-yl)methyl]thio}pyridine-3,5-dicarbonitrile ***17****.*

Yield 37%; preparative TLC, eluent EtOAC/cyclohexane/MeOH, 6:3:1); mp 260-262 °C (2-propanol/EtOAc); ^{1}H NMR (DMSO-d_6) 7.40 (d, 2H, Ar J = 8.5 Hz), 7.19 (s, 2H, NH_2), 7.12 (d, 2H, Ar J = 8.1 Hz), 6.44 (s, 1H, NH), 5.82 (s, 2H, SCH_2), 3.92 (d, 2H, OCH_2, J = 7.1 Hz), 3.77 (t, 2H, CH_2, J = 9.3 Hz), 3.23 (t, 2H, CH_2, J = 10.4 Hz), 1.31- 1.24 (m, 1H, CH), 0.68- 0.58 (m, 2H, CHeq), 0.35 – 0.30 (m, 2H, CHax). Anal. Calcd for $C_{21}H_{20}N_6OS$.

2-{[(1H-Benzo[d]imidazol-2-yl)methyl]thio}-6-amino-4-[4-(cyclopropylmethoxy)phenyl]pyridine-3,5-dicarbonitrile ***18****.*

Yield 64%; mp >300 °C (MeOH); ^{1}H NMR (DMSO-d_6) 12.3 (br s, 1H, NH), 7.9-8.4 (br s, 2H, NH_2), 7.57 (d, 1H, Ar, J= 7.8 Hz), 7.46-7.48 (m, 3H, Ar), 7.15-7.20 (m, 2H, Ar), 7.09 (d, 2H, ar, J= 8.7 Hz),

4.71 (s, 2H, CH_2), 3.9 (d, 2H, OCH_2, J= 7.1 Hz), 1.22-1.30 (m, 1H, CH), 0.57-0.62 (m, 2H, CHeq), 0.33-0.37 (m, 2H, CHax); IR 3396, 3331, 2210. Anal. Calcd for $C_{25}H_{20}N_6OS$.

2-{[(1H-Pyrazol-5-yl)methyl]thio}-6-amino-4-[4-(cyclopropylmethoxy)phenyl]pyridine-3,5-dicarbonitrile ***19***.

Yield 37%; mp 133-136 °C (EtOH/cyclohexane); ^{1}H NMR (DMSO-d_6) 12.7 (br s, 1H, NH), 8.0 (br s, 2H, NH_2), 7.67 (br s, 1H, Ar), 7.47 (d, 2H, Ar, J= 8.3 Hz), 7.09 (d, 2H, Ar, J= 8.5 Hz), 6.32 (s, 1H, Ar), 4.49 (s, 2H, SCH_2), 3.91 (d, 2H, OCH_2, J= 6.9), 1.22-1.26 (m, 1H, CH), 0.58-0.62 (m, 2H, CHeq), 0.36-0.40 (m, 2H, CHax). Anal. Calcd for $C_{21}H_{18}N_6OS$.

2-{[(1H-1,2,4-Triazol-5-yl)methyl]thio}-6-amino-4-[4-(cyclopropylmethoxy)phenyl]pyridine-3,5-dicarbonitrile ***20***.

Yield 72%; mp 240-242 °C (EtOH/Et_2O); ^{1}H NMR (DMSO-d_6) 13.9 (br s, 1H, NH), 8.3 (br s, 1H, Ar), 8.10 (br s, 2H, NH_2), 7.48 (d, 2H, Ar, J= 7.8 Hz), 7.09 (d, 2H, Ar, J= 8.5 Hz), 4.59 (s, 2H, SCH_2), 3.91 (d, 2H, OCH_2, J= 7.1 Hz), 1.23-1.29 (m, 1H, CH), 0.57-0.62 (m, 2H, CHeq), 0.34-0.37 (m, 2H, CHax); IR 3441, 3323, 3207, 2212. Anal. Calcd for $C_{20}H_{17}N_7OS$.

2-{[(1H-Tetrazol-5-yl)methyl]thio}-6-amino-4-[4-(cyclopropylmethoxy)phenyl]pyridine-3,5-dicarbonitrile ***21***.

Yield 64%; mp 225-227 °C (EtOH/Et_2O); ^{1}H NMR (DMSO-d_6) 16.10 (br s, 1H, NH), 8.00 (br s, 2H, NH_2), 7.47 (d, 2H, Ar, J= 8.6 Hz), 7.09 (d, 2H, Ar, J= 8.6 Hz), 4.78 (s, 2H, SCH_2), 3.91 (d, 2H, OCH_2, J= 7.0 Hz), 1.24-1.28 (m, 1H, CH), 0.58-0.61 (m, 2H, CHeq), 0.34-0.37 (m, 2H, CHax); IR 3442, 3323, 3224, 2225, 2208. Anal. Calcd for $C_{19}H_{16}N_8OS$.

2-Amino-6-{[(2-aminothiazol-4-yl)methyl]thio}-4-[4-(cyclopropylmethoxy)phenyl]pyridine-3,5-dicarbonitrile ***22***.

Yield 87%; mp 238-240 °C (EtOH/Et_2O); ^{1}H NMR (DMSO-d_6) 8.02 (br s, 2H, NH_2), 7.46 (d, 2H, Ar, J= 8.7 Hz), 7.08 (d, 2H, Ar, J= 8.7 Hz), 6.98 (br s, 2H, NH_2), 6.63 (s, 1H, Ar), 4.31 (s, 2H, SCH_2), 3.90 (d, 2H, OCH_2, J= 7.0 Hz), 1.23-1.29 (m, 1H, CH), 0.57-0.62 (m, 2H, CHeq), 0.34-0.37 (m, 2H, CHax); IR 3423, 3327, 3184-3170, 2216. Anal. Calcd for $C_{21}H_{18}N_6OS_2$.

2-{[(1H-1,2,4-Triazol-1-yl)methyl]thio}-6-amino-4-[4-(cyclopropylmethoxy)phenyl]pyridine-3,5-dicarbonitrile ***23***.

Yield 40%; mp 235-237 °C (EtOH); ^{1}H NMR (DMSO-d_6) 8.99 (s, 1H, Ar), 8.75 – 7.78 (m, 2H, NH_2), 8.04 (s, 1H, Ar), 7.47 (d, 2H, Ar, J= 8.7 Hz), 7.08 (d, 2H, Ar, J= 8.8 Hz), 6.03 (s, 2H, CH_2), 3.90 (d, 2H, CH_2, J = 7.1 Hz), 1.32- 1.24 (m, 1H, CH), 0.64- 0.54 (m, 2H, CHeq), 0.38-0.32 (m, 2H CHax); IR 3311, 2212. Anal. Calcd for $C_{20}H_{17}N_7OS$.

2-Amino-4-[4-(cyclopropylmethoxy)phenyl]-6-[(pyridin-3-ylmethyl)thio]pyridine-3,5-dicarbonitrile ***24***.

Yield 80%; mp 190-192 °C (MeOH); ^{1}H NMR (DMSO-d_6) 8.7 (s, 1H, Ar), 8.45 (s, 1H, Ar), 8.11 (br s, 2H, NH_2), 7.94 (d, 1H, Ar, J= 5.7 Hz), 7.42 (d, 2H, Ar, J= 6.8 Hz), 7.35-7.37 (m, 1H, Ar), 7.05 (d, 2H, ar, J= 6.9 Hz), 4.48 (s, 2H, SCH_2), 3.86 (d, 2H, OCH_2, J= 7.0 Hz), 1.19-1.25 (m, 1H, CH), 0.56-0.59 (m, 2H, CH eq), 0.30-0.34 (m, 2H, CH ax); IR 3369, 2212. Anal. Calcd for $C_{23}H_{19}N_5OS$.

2-{[6-Amino-3,5-dicyano-4-(4-ethoxyphenyl)pyridin-2-yl]thio}-N-methylacetamide ***25***.

Yield 32%; mp 262-264 °C (EtOH); ^{1}H NMR (DMSO-d_6) 8.1-7.9 (m, 3H, NH + NH_2), 7.48 (d, 2H, Ar, J= 8.5 Hz), 7.09 (d, 2H, Ar, J= 8.4 Hz), 4.12 (q, 2H, OCH_2, J= 7.2 Hz,), 3.88 (s, 2H, SCH_2), 2.61 (d, 3H, CH_3, J= 4.6 Hz), 1.36 (t, 3H, CH_3, J= 6.8 Hz); ^{13}C NMR (DMSO-d_6): 167.78, 166.54, 160.15, 158.57, 130.67, 126.05, 115.93, 114.94, 93.63, 86.73, 63.83, 33.71, 26.56, 15.07; IR 3394, 3223, 2210, 1637. Anal. Calcd for $C_{18}H_{17}N_5O_2S$.

2-{[(1H-Imidazol-2-yl)methyl]thio}-6-amino-4-(4-ethoxyphenyl)pyridine-3,5-dicarbonitrile ***26***.

Yield 41%; column chromatography, eluting system EtOAc/cyclohexane/MeOH, 6:3:1); mp 242-244 °C (EtOH); ^{1}H NMR (DMSO-d_6) 11.84 (s, 1H, NH), 8.1 (br s, 2H, NH_2), 7.47 (d, 2H, Ar, J= 8.6 Hz), 7.10-7.08 (m, 3H, Ar), 6.96 (s, 1H, Ar), 4.50 (s, 2H, SCH_2), 4.10 (q, 2H, OCH_2, J= 6.8 Hz), 1.36 (t, 3H, CH_3, J= 6.8 Hz); ^{13}C NMR (DMSO-d_6): 166.60, 160.65, 160.32, 158.56, 143.01, 130.67, 126.06, 115.94, 115.89, 114.94, 93.66, 86.40, 63.83, 27.23, 15.06; IR 3506, 3398, 3159, 2212. Anal. Calcd for $C_{19}H_{16}N_6OS$.

2-{[(1H-Pyrazol-5-yl)methyl]thio}-6-amino-4-(4-ethoxyphenyl)pyridine-3,5-dicarbonitrile ***27***.

Yield 29%; column chromatography, eluting system EtOAc/cyclohexane/MeOH, 5:5:1); mp 195-197 °C (EtOH); ^{1}H NMR (DMSO-d_6) 12.72 (s, 1H, NH), 8.05 (BR s, 2H, NH_2), 7.65 (s, 1H, Ar), 7.47 (d, 2H, Ar, J= 8.3 Hz), 7.08 (d, 2H, Ar, J= 8.4 Hz), 6.31 (s, 1H, Ar), 4.48 (s, 2H, SCH_2), 4.11 (q, 2H, OCH_2, J= 6.8 Hz), 1.36 (t, 3H, CH_3, J= 6.8 Hz); IR 3456, 3319, 3215, 2218. Anal. Calcd for $C_{19}H_{16}N_6OS$.

2-{[(1H-Pyrazol-5-yl)methyl]thio}-4-(4-(allyloxy)phenyl)-6-aminopyridine-3,5-dicarbonitrile ***28***.

Yield 65%; preparative TLC, eluent CH_2Cl_2/MeOH, 9.5:0.5); mp 129-131°C (EtOH); ^{1}H NMR (DMSO-d_6): 12.71 (br s, 1H, NH), 8.08 (br s, 2H, NH_2), 7.59 (br s, 1H, Ar), 7.49 (d, 2H, Ar, J= 8.7 Hz), 7.12 (d, 2H, Ar, J= 8.7 Hz), 6.32 (d, 1H, Ar, J = 2 Hz), 6.13-6.03 (m, 1H, CH), 5.44 (dd, 1H, CH, J= 17.3, 1.6 Hz), 5.30 (d, 1H, CH, J= 10.4 Hz), 4.66 (d, 2H, OCH_2, J= 5.2 Hz), 4.49 (s, 2H, SCH_2); ^{13}C NMR (DMSO-d_6): 160.25, 160.23, 158.49, 133.86, 130.67, 128.81, 126.41, 125.65, 118.35, 115.95, 115.18, 111.08, 109.95, 105.12, 93.71, 86.31, 68.84; IR 3335, 3179, 2210. Anal. Calcd for $C_{20}H_{16}N_6OS$.

4-(Cyclobutylmethoxy)benzaldehyde 29 [35].

To a solution of 4-hydroxybenzaldehyde (12.3 mmol) in anhydrous acetone (20 mL), potassium carbonate (18.5 mmol) was added, followed by the cyclobutylmethyl bromide (18.5 mmol). The mixture was heated at reflux for 36 h. Then, the mixture was cooled to rt and the insoluble material was filtered and washed with acetone (3 x 20 mL). The resulting filtrates were collected and evaporated under vacuum, affording an oily residue which was dissolved in EtOAc (150 mL). The organic layer was washed with 25% NaOH solution (4x30 mL), with water (3x30 mL) and then dried (Na_2SO_4). After evaporation of the solvent, the desired compound was obtained as a viscous oil. The product was pure enough to be used without further purification. Yield 67%; ^{1}H NMR (DMSO-d_6) 9.86 (s, 1H, CHO), 7.85 (d, 2H, Ar, J= 8.8 Hz), 7.11 (d, 2H, Ar, J= 8.4 Hz), 4.06 (d, 2H, OCH_2, J= 6.8 Hz), 2.77-2.71 (m, 1H, CH), 2.08-2.07 (m, 2H, CH_2), 1.90-1.82 (m, 4H, $2CH_2$).

N-[4-(2,2-Dicyanovinyl)phenyl]acetamide 36 [37].

Malononitrile (17.3 mmol) and piperidine (two drops) were added to a solution of commercially available 4-acetamidobenzaldehyde **34** (17.3 mmol) in EtOH (20 mL). The mixture was heated at reflux for 2h, then cooled to rt affording an orange solid which was filtered, washed with Et_2O (5 mL) and petroleum ether (2 ml), and recrystallized. Yield 63%; mp 234-236 °C (EtOH); ^{1}H NMR (DMSO-d_6) 10.51 (s, 1H, NH), 8.37 (s, 1H, CH), 7.94 (d, 2H, Ar, J= 8.4 Hz), 7.80 (d, 2H, Ar, J= 8.8 Hz), 2.11 (s, 3H, CH_3); IR 2224, 1693. Anal. Calcd for $C_{12}H_9N_3O$.

General Procedure for the Synthesis of 2-Amino-4-Aryl-6-(phenylthio)pyridine-3,5-dicarbonitriles 37-41, 43.

To a stirred solution of the suitable aldehyde **29** [35], **30-33**, **35** (10 mmol), malononitrile (20 mmol) and DBU (5% mol) in 10% aqueous EtOH (20 mL), thiophenol (10 mmol) was added after 20 min. Thus, the reaction mixture was stirred at 55°C until the disappearance of the starting material (TLC monitoring). The suspension was then cooled to rt and a solid precipitated which was collected by filtration, washed with Et_2O (5-10 mL) and then dried in oven at 60 °C overnight. The crude products were purified by crystallization.

*2-Amino-4-[4-(cyclobutylmethoxy)phenyl]-6-(phenylthio)pyridine-3,5-dicarbonitrile **37**.*

Yield 18%; mp 180-182 °C (MeOH); ^{1}H NMR (DMSO-d_6) 7.7 (br s, 2H, NH_2), 7.61-7.60 (m, 2H, Ar), 7.51-7.49 (m, 5H, Ar), 7.12 (d, 2H, Ar, J = 8.6 Hz), 4.05 (d, 2H, OCH_2, J = 6.5 Hz), 2.77-2.75 (m, 1H, CH), 2.11-2.09 (m, 2H, CH_2), 1.93-1.89 (m, 4H, $2CH_2$); IR 3348, 3280, 2216. Anal. Calcd for $C_{24}H_{20}N_4OS$.

*2-Amino-4-(4-isobutoxyphenyl)-6-(phenylthio)pyridine-3,5-dicarbonitrile **38**.*

Yield 26%; mp 181-183 °C (MeOH); ^{1}H NMR (DMSO-d_6) 7.74 (s, 2H, NH_2), 7.61-7.59 (m, 2H, ar), 7.50-7.49 (m, 5H, Ar), 7.11 (d, 2H, Ar, J= 8.8 Hz), 3.84 (d, 2H, OCH_2, J= 6.4 Hz), 2.09-2.02 (m, 1H, CH), 1.02 (s, 3H, CH_3), 1.00 (s, 3H, CH_3); IR 3302, 3232, 2214. Anal. Calcd for $C_{23}H_{20}N_4OS$.

*2-Amino-4-(4-ethoxyphenyl)-6-(phenylthio)pyridine-3,5-dicarbonitrile **39**.*

Yield 37%; mp 252-254 °C (2-propanol); ^{1}H NMR (DMSO-d_6) 7.60 (s, 2H, NH_2), 7.62-7.60 (m, 2H, Ar), 7.58-7.48 (m, 5H, Ar), 7.11 (d, 2H, Ar, J= 8.8 Hz), 4.13 (q, 2H, OCH_2, J= 6.8 Hz), 1.37 (t, 3H, CH_3, J= 7.2 Hz); IR 3344, 3215, 2216. Anal. Calcd for $C_{21}H_{16}N_4OS$.

4-[4-(Allyloxy)phenyl]-2-amino-6-(phenylthio)pyridine-3,5-dicarbonitrile ***40***.

Yield 28%; mp 234-236 °C (EtOAc/cyclohexane); ^{1}H NMR (DMSO-d_6): 7.77 (s, 2H, NH_2), 7.61-7.60 (m, 2H, Ar), 7,59-7.58 (m, 3H, Ar), 7.51 (d, 2H, Ar, J= 8.8 Hz), 7.14 (d, 2H, Ar, J= 8.8 Hz), 6.13-6.03 (m, 1H, CH), 5.45 (dd, 1H, CH, J=17.2, 1.6 Hz), 5.30 (d, 1H, CH, J=10.5Hz), 4.67 (d, 2H, OCH_2, J= 5.6 Hz); IR 3358, 3215, 2214, 1624. Anal. Calcd for $C_{22}H_{16}N_4OS$.

2-Amino-4-{4-[(2-methylallyl)oxy]phenyl}-6-(phenylthio)pyridine-3,5-dicarbonitrile ***41***.

Yield 25%; mp 198-200 °C (EtOH); ^{1}H NMR (DMSO-d_6) 7.76 (s, 2H, NH_2), 7.60-7.61 (m, 2H, ar), 7.60-7.59 (m, 3H, Ar), 7.55 (d, 2H, Ar, J= 8.4 Hz), 7.14 (d, 2H, Ar, J= 8.4 Hz), 5.11 (d, 1H, CH), 5.00 (d, 1H, CH), 4.58 (s, 2H, CH_2), 1.81 (s, 3H, CH_3); IR 3481, 3369, 2212. Anal. Calcd for $C_{23}H_{18}N_4OS$.

2-Amino-4-[4-(cyclopropylmethoxy)phenyl]-6-(phenylthio)pyridine-3,5-dicarbonitrile ***43***.

Yield 33%; mp 261-263 °C (EtOH); ^{1}H NMR (DMSO-d_6) 7.70 (br s, 2H, NH_2), 7.60-7.62 (m, 2H, Ar), 7.48-7.51 (m, 5H, Ar), 7.10 (d, 2H, Ar, J = 8.1 Hz), 3.92 (d, 2H, CH_2, J = 7.8 Hz), 1.25-1.28 (m, 1H, CH), 0.58-0.62 (m, 2H, 2CH*eq*), 0.36-0.38 (m, 2H, 2CH*ax*); IR 3330, 3220, 2224. Anal. Calcd for $C_{23}H_{18}N_4OS$.

N-{4-[2-Amino-3,5-dicyano-6-(phenylthio)pyridin-4-yl]phenyl}acetamide 42 [37].

A solution of compound **36** [37] (5.4 mmol), malononitrile (5.4 mmol), thiophenol (5.4 mmol) and Et_3N (0.54 mmol) in EtOH (30 mL) was heated at reflux for 2h. Then, after cooling to rt a yellow solid was obtained which was filtered and washed with Et_2O (5 mL). Yield 44%; mp > 300°C (EtOH); ^{1}H NMR (DMSO-d_6) 10.24 (s, 1H, NH), 7.76 (s, 2H, NH_2), 7.74 (m, 2H, Ar), 7.61-7.60 (m, 5H, Ar), 7.50 (d, 2H, Ar, J= 8.0 Hz), 2.10 (s, 3H, CH_3); IR 3481, 3344, 3298, 2212, 1681. Anal. Calcd for $C_{21}H_{15}N_5OS$.

General Procedure For the Synthesis of 2-Amino-4-Aryl-6-mercaptopyridine-3,5-dicarbonitriles 44-50.

To a stirred solution of the suitable 6-phenylsulfanyl derivative **37-43** (10 mmol) in anhydrous DMF (1 mL) maintained at rt and under nitrogen atmosphere, an excess of sodium sulfite (33 mmol) was added. The reaction mixture was heated at 80 °C for 2 h. Then, 1N HCl (25 mL) was added followed by addition of 6N HCl (5 mL) to obtain a huge precipitate which was filtered and washed with water (20 mL) and Et_2O (5 mL). The crude derivatives were purified by crystallization.

*2-Amino-4-[4-(cyclobutylmethoxy)phenyl]-6-mercaptopyridine-3,5-dicarbonitrile **44**.*

Yield 84%; mp 256-259 °C (EtOH); ^{1}H NMR (DMSO-d_6) 12.95 (s, 1H, SH), 7.08 (s, 2H, NH_2), 7.46 (d, 2H, Ar, J= 8.0 Hz), 7.09 (d, 2H, Ar, J= 8.4 Hz), 4.04 (d, 2H, OCH_2, J= 6 Hz), 2.87-2.73 (m, 1H, CH), 2.10-1.92 (m, 2H, CH_2), 1.90-1.89 (m, 4H, $2CH_2$); IR 3474, 3335, 2214. Anal. Calcd for $C_{18}H_{16}N_4OS$.

*2-Amino-4-(4-isobutoxyphenyl)-6-mercaptopyridine-3,5-dicarbonitrile **45**.*

Yield 86%; mp 210-213 °C (EtOH); ^{1}H NMR (DMSO-d_6) 13.02 (s, 1H, SH), 7.77 (s, 2H, NH_2), 7.45 (d, 2H, Ar, J= 8.8 Hz), 7.09 (d, 2H, Ar, J= 8.4 Hz), 3.83 (d, 2H, CH_2, J= 6.4 Hz), 2.06-2.03 (m, 1H, CH), 1.02 (s, 3H, CH_3), 0.99 (s, 3H, CH_3). Anal. Calcd for $C_{17}H_{16}N_4OS$.

*2-Amino-4-(4-ethoxyphenyl)-6-mercaptopyridine-3,5-dicarbonitrile **46*** [38].

Yield 76%; mp: 290-292 °C (EtOH); ^{1}H NMR (DMSO-d_6) 12.99 (s, 1H, SH), 8.11 (s, 2H, NH_2), 7.54 (d, 2H, Ar, J= 8.8 Hz), 7.14 (d, 2H, Ar, J= 8.8 Hz), 4.14 (q, 2H, CH_2, J= 6.8 Hz), 1.38 (t, 3H, CH_3, J= 6.8 Hz); IR 3336, 3117, 2212. Anal. Calcd for $C_{15}H_{12}N_4OS$.

*4-[4-(Allyloxy)phenyl]-2-amino-6-mercaptopyridine-3,5-dicarbonitrile **47*** [13].

Yield 84%; mp 208-211 °C (EtOAc); ^{1}H NMR (DMSO-d_6) 12.98 (s, 1H, SH); 7.90 (s, 2H, NH_2); 7.47 (d, 2H, Ar, J= 8.6 Hz); 7.12 (d, 2H, Ar, J= 8.6 Hz); 6.11-6.04 (m, 1H, CH); 5.45 (dd, 1H, CH, J= 17.2, 1.2 Hz,), 5.30 (dd, 1H, CH, J= 10.4, 1.2 Hz), 4.66 (d, 2H, OCH_2, J= 5.6 Hz,); IR 3476, 3319, 3209, 2212. Anal. Calcd for $C_{16}H_{12}N_4OS$.

*2-Amino-6-mercapto-4-{4-[(2-methylallyl)oxy]phenyl}pyridine-3,5-dicarbonitrile **48**.*

Yield 72%; mp 180-183 °C dec. (EtOH); ^{1}H NMR (DMSO-d_6) 12.98 (s, 1H, SH), 8.11 (br s, 2H, NH_2), 7.53 (d, 2H, Ar, J= 7.4 Hz), 7.08 (d, 2H, Ar, J= 8.8), 5.09 (s, 1H, CH), 4.90 (s, 1H, CH), 4.58 (s, 2H, OCH_2), 1.80 (s, 3H, CH_3). Anal. Calcd for $C_{17}H_{14}N_4OS$.

*N-[4-(2-amino-3,5-dicyano-6-mercaptopyridin-4-yl)phenyl]acetamide **49*** [37].

Yield 40%; mp 275-277 °C dec. (EtOH/EtOAc); ^{1}H NMR (DMSO-d_6) 12.94 (s, 1H, SH), 10.37 (s, 1H, NH), 8.19 (s, 2H, NH_2), 7.73 (d, 2H, Ar, J= 8.0 Hz), 7.44 (d, 2H, Ar, J= 8.0 Hz), 2.08 (s, 3H, CH_3); IR 3317, 3215, 2214, 1539. Anal. Calcd for $C_{15}H_{11}N_5OS$.

*2-Amino-4-[4-(cyclopropylmethoxy)phenyl]-6-mercaptopyridine-3,5-dicarbonitrile **50**.*

Yield 80%; mp 168-170 °C (EtOAc); ^{1}H NMR (DMSO-d_6) 12.9 (br s, 1H, SH), 7.8 (br s, 2H, NH_2), 7.45 (d, 2H, Ar, J = 8 Hz), 7.08 (d, 2H, Ar, J = 8 Hz), 3.91 (d, 2H, CH_2, J = 7.8 Hz), 1.23-1.27 (m, 1H, CH), 0.57-0.62 (m, 2H, CHeq), 0.33-0.37 (m, 2H, CHax); IR 3309, 3190, 2219. Anal. Calcd for $C_{17}H_{14}N_4OS$.

2-Chloro-N-hydroxyacetamide 51 [39].

An aqueous 50 % solution of hydroxylamine (12.0 mmol) was added to ethyl chloroacetate (12.0 mmol) in a 50 ml round bottomed flask and stirred for 5 min at rt. Then, the mixture was cooled at 4 °C and stirred for 15 min, and finally, re-warmed to rt and stirred for 3 h. The resulting precipitate was collected by filtration and used for the next step without any further purification. Yield 53%; mp 93-95 °C (Lit mp 92-93 °C); ^{1}H NMR (DMSO): 7.41 (br s, 2H, OH + NH), 3.94 (s, 2H, CH_2).

3,6-Diamino-5-cyano-4-[4-(cyclopropylmethoxy)phenyl]thieno[2,3-b]pyridine-2-carboxamide 52.

A solution of compound **1** [13,21] (0.71 mmol) and potassium hydroxide (1.42 mmol) in absolute EtOH (10 mL) was refluxed for 3h. Then, iced-water (30 mL) was added and the mixture was neutralized with 5N HCl. The green solid was collected by filtration, washed with water (10 ml) and

with Et_2O (5 mL), and then recrystallized. Yield 85%; mp 260-262 °C (Dioxane); ^{1}H NMR (DMSO-d_6) 7.39 (d, 2H, Ar, J= 8.0 Hz), 7.27 (br s, 2H, NH_2), 7.12 (d, 2H, Ar, J= 8.4 Hz), 6.96 (br s, 2H, NH_2), 5.70 (s, 2H, NH_2), 3.91 (d, 2H, OCH_2, J= 6.8 Hz), 1.30-1.23 (m, 1H, CH), 0.62-0.58 (m, 2H, CHeq), 0.38-0.34 (m, 2H, CHax); ^{13}C NMR (DMSO-d_6): 167.23, 163.83, 160.08, 158.93, 152.76, 146.75, 130.06, 125.74, 116.43, 115.29, 114.78, 93.35, 90.92, 72.71, 10.57, 3.62; IR 3466, 3452, 3346, 3315, 3136, 2214, 1629. Anal. Calcd for $C_{19}H_{17}N_5O_2S$.

Pharmacology

Cell culture and membrane preparation. CHO cells transfected with hA_1, hA_{2A}, hA_{2B} and hA_3 ARs were grown adherently and maintained in Dulbecco's modified Eagle's medium with nutrient mixture F12, containing 10% fetal calf serum, penicillin (100 U/ml), streptomycin (100 μg/ml), l-glutamine (2 mM), geneticine (G418; 0.2 mg/ml) at 37°C in 5% CO_2/95% air until the use in cAMP assays [54]. For membrane preparation the culture medium was removed, and the cells were washed with phosphate-buffered saline and scraped off T75 flasks in ice-cold hypotonic buffer (5 mM Tris HCl, 1 mM EDTA, pH 7.4). The cell suspension was homogenized with a Polytron, centrifuged for 30 min at 40000 *g* at 4°C and the resulting membrane pellet was used for competition binding experiments [54].

Competition binding experiments. All synthesized compounds have been tested for their affinity to hA_1, hA_{2A} and hA_3 ARs. Competition experiments to hA_1 ARs were carried out incubating 1 nM [^{3}H]-8-cyclopentyl-1,3-dipropylxanthine ([^{3}H]-DPCPX) with membrane suspension (50 μg of protein/100 μl) and different concentrations of the examined compounds at 25°C for 90 min in 50 mM Tris HCl, pH 7.4. Non-specific binding was defined as binding in the presence of 1 μM DPCPX and was always < 10% of the total binding [54]. Inhibition experiments to hA_{2A} ARs were performed incubating the radioligand [^{3}H]-ZM241385 (1 nM) with the membrane suspension (50 μg of protein/100 μl) and different concentrations of the examined compounds for 60 min at 4°C in 50 mM Tris HCl (pH 7.4), 10 mM $MgCl_2$. Non-specific binding was determined in the presence of ZM241385 (1 μM) and was

about 20% of the total binding [55]. Competition binding experiments to A_3 ARs were carried out incubating the membrane suspension (50 μg of protein/100 μl) with 0.5 nM [^{125}I]-N^6-(4-aminobenzyl)-*N*-methylcarboxamidoadenosine **(**[^{125}I]-ABMECA) in the presence of different concentration of the examined compounds for an incubation time of 120 min at 4°C in 50 mM Tris HCl (pH 7.4), 10 mM $MgCl_2$, 1 mM EDTA. Non-specific binding was defined as binding in the presence of 1μM ABMECA and was always < 10% of the total binding [56]. Bound and free radioactivity were separated by filtering the assay mixture through Whatman GF/B glass fiber filters using a Brandel cell harvester (Brandel Instruments, Unterföhring, Germany). The filter bound radioactivity was counted by Packard Tri Carb 2810 TR scintillation counter (Perkin Elmer).

Cyclic AMP assays. CHO cells transfected with hAR subtypes were washed with phosphate-buffered saline, detached with tripsine and centrifuged for 10 min at 200 g. Cells were seeded in 96-well white half-area microplate (Perkin Elmer, Boston, USA) in a stimulation buffer composed of Hank Balanced Salt Solution, 5 mM HEPES, 0.5 mM Ro 20-1724, 0.1% BSA. The examined compounds (1 nM - 1μM) were tested alone and/or in the presence of NECA, 100 nM. cAMP levels were then quantified by using the AlphaScreen cAMP Detection Kit (Perkin Elmer, Boston, USA) following the manufacturer's instructions [57]. At the end of the experiments, plates were read with the Perkin Elmer EnSight Multimode Plate Reader.

Data Analysis. The protein concentration was determined according to a Bio-Rad method with bovine albumin as a standard reference. Inhibitory binding constant (K_i) values were calculated from those of IC_{50} according to Cheng & Prusoff equation $K_i = IC_{50}/(1+[C^*]/K_D^*)$, where [C*] is the concentration of the radioligand and K_D* its dissociation constant [56]. K_i and IC_{50} values were calculated by non-linear regression analysis using the equation for a sigmoid concentration-response curve (Graph-PAD Prism, San Diego, CA, U.S.A).

Molecular Modelling

Homology modelling and energy minimization studies were carried out using MOE (Molecular Operating Environment, version 2014.09) suite [47]. All ligand structures were optimized using RHF/AM1 semiempirical calculations and the software package MOPAC [48] implemented in MOE was used for these calculations.

Homology modelling of the hA_{2B} AR. Homology models of the hA_{2B} AR were built using recently solved X-ray structures of the hA_{2A} AR in complex with Ado and UK-432097 as templates, both structures being retrieved from Protein Data Bank (pdb code: 2YDO; 3.0-Å resolution [45] and pdb code: 3QAK; 2.7-Å resolution [46], respectively). A multiple alignment of the hAR primary sequences was built within MOE as preliminary step. For all hA_{2B} AR models, the boundaries identified from the used X-ray crystal structure of hA_{2A} AR were then applied for the corresponding sequences of the TM helices of the hA_{2B} AR. The missing loop domains were built by the loop search method implemented in MOE. Once the heavy atoms were modelled, all hydrogen atoms were added, and the protein coordinates were then minimized with MOE using the AMBER99 force field [58] until the Root Mean Square (RMS) gradient of the potential energy was less than 0.05 kJ mol^{-1} $Å^{-1}$. Reliability and quality of these models were checked using the Protein Geometry Monitor application within MOE, which provides a variety of stereochemical measurements for inspection of the structural quality in a given protein, like backbone bond lengths, angles and dihedrals, Ramachandran φ-ψ dihedral plots, and quality of side chain rotamer and non-bonded contact.

Molecular docking analysis. All compound structures were docked into the binding site of the hA_{2B} AR structures using three docking tools: the Induced Fit docking protocol of MOE, the genetic algorithm docking tool of CCDC Gold [49], and the Lamarckian genetic algorithm of Autodock [50,51]. The Induced Fit docking protocol of MOE is divided into several stages: *Conformational Analysis of ligands*. The algorithm generated conformations from a single 3D conformation by conducting a systematic search. In this way, all combinations of angles were created for each ligand. *Placement*. A collection of poses was generated from the pool of ligand conformations using Alpha Triangle placement method. Poses were generated by superposition of ligand atom triplets and triplet

points in the receptor binding site. The receptor site points are alpha sphere centres which represent locations of tight packing. At each iteration, a random conformation was selected, a random triplet of ligand atoms and a random triplet of alpha sphere centres were used to determine the pose. *Scoring*. Poses generated by the placement methodology were scored using the *Alpha HB* scoring function, which combines a term measuring the geometric fit of the ligand to the binding site and a term measuring hydrogen bonding effects. *Induced Fit*. The generated docking conformations were subjected to energy minimization within the binding site and the protein sidechains are included in the refinement stage. In detail, the protein backbone is set as rigid while the side chains are not set to "free to move" but are set to "tethered", where an atom tether is a distance restraint that restrains the distance not between two atoms but between an atom and a fixed point in space. *Rescoring*. Complexes generated by the Induced Fit methodology stage were scored using the *Alpha HB* scoring function. Gold tool was used with default efficiency settings through MOE interface, by selecting GoldScore as scoring function [49]. Autodock 4.2.6 software was used with PyRx interface. Lamarckian genetic algorithm was employed for this analysis with the following settings: 50 runs for each ligand; 2,500,000 as maximum number of energy evaluations; 27,000 as maximum number of generations; 0.02 as rate of gene mutation and 0.8 as rate of crossover. The grid box was set with 50, 50, and 50 points in the *x*, *y*, and *z* directions, respectively, with the default grid spacing of 0.375 Å [50,51,59].

ASSOCIATED CONTENT

Supporting information

Combustion analysis data of the newly synthesized compounds; comparison of the docking conformation of compound **15** at the two A_{2B} AR models binding cavity; Description of the alternative binding mode for the analyzed compounds at the A_{2B} AR binding cavity.

Notes

All authors materially participated in the research and article preparation. All authors have approved the final article and declare no competing financial interest.

ACKNOWLEDGMENTS

The work was financially supported by the Italian Ministry for University and Research (MIUR, PRIN 2010-2011, 20103W4779_004 project) and the University of Florence.

REFERENCES

[1] K.A. Jacobson, L.J.S. Knutsen, P1 and P2 purine and pyrimidine receptor ligands, in: M.P. Abbracchio, M. Williams (Eds.), Purinergic and Pyrimidinergic Signalling, Handbook of experimental Pharmacology, Berlin, 2001, Vol. 151/1, pp. 129-175.

[2] P.A. Borea, S. Gessi., S. Merighi, K. Varani, Adenosine as multi-signalling guardian angel in human diseases: when, where and how oes it exert its protective effects? Trends Pharmacol. Sci. 37 (2016) 419-434.

[3] C.E. Müller, K.A. Jacobson, Recent developments in adenosine receptor ligands and their potential as novel drugs, Biochim. Biophys. Acta 1808 (2011) 1290-1308.

[4] J. Zablocki, E. Elzein, R. Kalla, A_{2B} adenosine receptor antagonists and their potential indications, Expert Opin. Ther. Pat. 16 (2006) 1347-1357.

[5] G. Ortore, A. Martinelli, A_{2B} receptor ligands: past, present and future trends, Curr. Top. Med. Chem. 10 (2010) 923-940.

[6] R.V. Kalla, J. Zablocki, Progress in the discovery of selective, high affinity A_{2B} adenosine receptor antagonists as clinical candidates, Purinergic Signal. 5 (2009) 21-29.

[7] A. Carotti, M.I. Cadavid, N.B. Centeno, C. Esteve, M.I. Loza, A. Martinez, R. Nieto, E. Ravina, F. Sanz, V. Segarra, E. Sotelo, A. Stefanachi, B. Vidal, Design, synthesis, and structure-activity

relationships of 1-,3-,8-, and 9-substituted-9-deazaxanthines at the human A_{2B} adenosine receptor, J. Med. Chem. 49 (2006) 282-299.

[8] A.W. Cheung, J. Brinkman, F. Firooznia, A. Flohr, J. Grimsby, M.L. Gubler, K. Guertin, R. Hamid, N. Marcopulos, R.D. Norcross, L. Qi, G. Ramsey, J. Tan, Y. Wen, R. Sarabu, 4-Substituted-7-N-alkyl-N-acetyl 2-aminobenzothiazole amides: drug-like and non-xanthine based A_{2B} adenosine receptor antagonists, Bioorg. Med. Chem. Lett. 20 (2010) 4140-4146.

[9] P. Eastwood, J. Gonzalez, S. Paredes, S. Fonquerna, A. Cardus, J.A. Alonso, A. Nueda, T. Domenech, R.F. Reinoso, B. Vidal, Discovery of potent and selective bicyclic A_{2B} adenosine receptor antagonists via bioisosteric amide replacement, Bioorg. Med. Chem. Lett. 20 (2010) 1634-1637.

[10] A. El Maatougui, J. Azuaje, M. Gonzalez-Gomez, G. Miguez, A. Crespo, C. Carbajales, L. Escalante, X. Garcia-Mera, H. Gutierrez-de-Teran, E. Sotelo, Discovery of Potent and Highly Selective A_{2B} Adenosine Receptor Antagonist Chemotypes, J. Med. Chem. 59 (2016) 1967-1983.

[11] P.G. Baraldi, M.A. Tabrizi, F. Fruttarolo, R. Romagnoli, D. Preti, Recent improvements in the development of A_{2B} adenosine receptor agonists, Purinergic Signal. 5 (2009) 3-19.

[12] P.G. Baraldi, D. Preti, M.A. Tabrizi, F. Fruttarolo, R. Romagnoli, M.D. Carrion, L.C. Cara, A.R. Moorman, K. Varani, P.A. Borea, Synthesis and biological evaluation of novel 1-deoxy-1-[6-[((hetero)arylcarbonyl)hydrazino]- 9*H*-purin-9-yl]-*N*-ethyl-β-D-ribofuranuronamide derivatives as useful templates for the development of A_{2B} adenosine receptor agonists, J. Med. Chem. 50 (2007) 374-380.

[13] U. Rosentreter, R. Henning, M. Bauser, T. Krämer, A. Vaupel, W. Hübsch, K. Dembowsky, O. Salcher-Schraufstätter, J.P. Stasch, T. Krahn, E. Perzborn, Substituted 2-Thio-3,5-Dicyano-4-Aryl-6-Aminopyridines and the use Thereof as Adenosine Receptor Ligands, 2001, WO/2001/025210.

[14] D. Van der Hoeven, T.C. Wan, E.T. Gizewski, L.M. Kreckler, J.E. Maas, J. Van Orman, K. Ravid, J.A. Auchampach, Arole for the low-affinity A_{2B} adensine receptor in regulating superoxide generation by murine neutrophils. J. Pharmacol. Exp. Ther. 338 (2011) 1004-1012.

[15] I. Feoktistov, I. Biaggioni, Role of adenosine in asthma, Drug Dev. Res. 39 (1996) 333-336.

[16] C.N. Wilson, A. Nadeem, D. Spina, R. Brown, C.P. Page, S.J. Mustafa, Adenosine receptors and asthma, Handb. Exp. Pharmacol. (2009) 329-362.

[17] R. Walaschewski, F. Begrow, E.J. Verspohl, Impact and benefit of A_{2B} adenosine receptor agonists for the respiratory tract: mucociliary clearance, ciliary beat frequency, trachea muscle tonus and cytokine release, J. Pharm. Pharmacol. 65 (2013) 123-132.

[18] H. Karmouty-Quintana, H. Zhong, L. Acero, T. Weng, E. Melicoff, J.D. West, A. Hemnes, A. Grenz, H.K. Eltzschig, T.S. Blackwell, Y. Xia, R.A. Johnston, D. Zeng, L. Belardinelli, M.R. Blackburn, The A_{2B} adenosine receptor modulates pulmonary hypertension associated with interstitial lung disease, FASEB J. 26 (2012) 2546–2557.

[19] T. Eckle, T. Krahn, A. Grenz, D. Kohler, M. Mittelbronn, C. Ledent, M.A. Jacobson, H. Osswald, L.F. Thompson, K. Unertl, H.K. Eltzschig, Cardioprotection by ecto-5'-nucleotidase (CD73) and A_{2B} adenosine receptors, Circulation 115 (2007) 1581-1590.

[20] S. Toldo, H. Zhong, E. Mezzaroma, B.W. Van Tassell, H. Kannan, D. Zeng, L. Belardinelli, N.F. Voelkel, A. Abbate, GS-6201, a selective blocker of the A_{2B} adenosine receptor, attenuates cardiac remodeling after acute myocardial infarction in the mouse, J. Pharmacol. Exp. Ther. 343 (2012) 587-595.

[21] T. Krahn, T. Kramer, U. Rosentreter, J.M. Downey, N. Solenkova, Use of substituted 2-thio-3,5-dicyano-4-phenyl-6-aminopyridines for the treatment of reperfusion injury and reperfusion damage, 2006, WO2006099958A1.

[22] A. Kuno, S.D. Critz, L. Cui, V. Solodushko, X.M. Yang, T. Krahn, B. Albrecht, S. Philipp, M.V. Cohen, J.M. Downey, Protein kinase C protects preconditioned rabbit hearts by increasing

sensitivity of adenosine A_{2B}-dependent signaling during early reperfusion, J. Mol. Cell. Cardiol. 43 (2007) 262-271.

[23] C. Lemos, B.S. Pinheiro, R.O. Beleza, J.M. Marques, R.J. Rodrigues, R.A. Cunha, D. Rial, A. Kofalvi, Adenosine A_{2B} receptor activation stimulates glucose uptake in the mouse forebrain, Purinergic Signal. 11 (2015) 561-569.

[24] H. Johnston-Cox, M. Koupenova, D. Yang, B. Corkey, N. Gokce, M.G. Farb, N. LeBrasseur, K. Ravid, The A_{2B} adenosine receptor modulates glucose homeostasis and obesity, PLoS One 7 (2012) e40584.

[25] R.A. Figler, G. Wang, S. Srinivasan, D.Y. Jung, Z. Zhang, J.S. Pankow, K. Ravid, B. Fredholm, C.C. Hedrick, S.S. Rich, J.K. Kim, K.F. LaNoue, J. Linden, Links between insulin resistance, adenosine A_{2B} receptors, and inflammatory markers in mice and humans, Diabetes 60 (2011) 669-679.

[26] S. Ryzhov, S.V. Novitskiy, R. Zaynagetdinov, A.E. Goldstein, D.P. Carbone, I. Biaggioni, M.M. Dikov, I. Feoktistov, Host A_{2B} adenosine receptors promote carcinoma growth, Neoplasia 10 (2008) 987-995.

[27] Q. Wei, S. Costanzi, R. Balasubramanian, Z.G. Gao, K.A. Jacobson, A_{2B} adenosine receptor blockade inhibits growth of prostate cancer cells, Purinergic Signal. 9 (2013) 271-280.

[28] M.A. Zimmerman, A. Grenz, E. Tak, M. Kaplan, D. Ridyard, K.S. Brodsky, M.S. Mandell, I. Kam, H.K. Eltzschig, Signaling through hepatocellular A_{2B} adenosine receptors dampens ischemia and reperfusion injury of the liver, Proc. Natl. Acad. Sci. U. S. A. 110 (2013) 12012-12017.

[29] Z.G. Gao, R. Balasubramanian, E. Kiselev, Q. Wei, K.A. Jacobson, Probing biased/partial agonism at the G protein-coupled A_{2B} adenosine receptor, Biochem. Pharmacol. 90 (2014) 297-306.

[30] M. W. Beukers, L.C.W. Chang, J. K. von Frijtag Drabbe Kunzel, T. Mulder-Krieger, R. F. Spanjersberg, J. Brussee, A.P. IJzermann, New, non-adenosine, high-potency agonists for the

human adenosine A_{2B} receptor with an improved selectivity profile compared to the reference agonist N-ethylcarboxamidoadenosine. J. Med. Chem. 47 (2004) 3707–3709.

[31] S. Hinz, S.K. Lacher, B.F. Seibt, C.E. Müller, BAY60-6583 acts as a partial agonist at adenosine A_{2B} receptors, J. Pharmacol. Exp. Ther. 349 (2014) 427-436.

[32] J.A. Baltos, E.A. Vecchio, M.A. Harris, C.X. Qin, R.H. Ritchie, A. Christopoulos, P.J. White, L.T. May, Capadenoson, a clinically trialed partial adenosine A_1 receptor agonist, can stimulate adenosine A_{2B} receptor biased agonism, Biochem. Pharmacol. 135 (2017) 79-89.

[33] L.C. W.Chang, J.K. von Frijtag Drabbe Künzel, T. Mulder-Krieger, R.F. Spanjersberg, S.F. Roerink, G. van den Hout, M.W. Beukers, J. Brussee, A.P. IJzerman, A series of ligand displaying a remarkable agonistic-antagonistic profile at the adenosine A_1 receptor. J. Med. Chem. 48 (2005) 2045-2053.

[34] D. Meibom, B. Albrecht-Kupper, N. Diedrichs, W. Hubsch, R. Kast, T. Kramer, U. Krenz, H.G. Lerchen, J. Mittendorf, P.G. Nell, F. Sussmeier, A. Vakalopoulos, K. Zimmermann, Neladenoson Bialanate Hydrochloride: A Prodrug of a Partial Adenosine A_1 Receptor Agonist for the Chronic Treatment of Heart Diseases, ChemMedChem 12 (2017) 728-737.

[35] S. Okuyama, H. Oono, M. Kawamura, Preparation of benzylidene rhodanine derivatives for lowering blood sugar, 1995, JP07070095 A 19950314.

[36] R. Mamgain, R. Singh, D.S. Rawat, DBU-catalyzed three-component one-pot synthesis of highly functionalized pyridines in aqueous ethanol, J. Het. Chem. 46 (2009) 69-73.

[37] U. Rosentreter, T. Krämer, M. Shimada, W. Hübsch, N. Diedrichs, T. Krahn, K. Henninger, J.P. Stasch, Substituted 2-thio-3,5-dicyano-4-phenyl-6-aminopyridines and their use as adenosine receptor-selective ligands, 2003, WO/2003/008384.

[38] A. Vakalopoulos, D. Meibom, P. Nell, F. Suessmeier, B. Albrecht-Kupper, K. Zimmerman, J. Keldenich, D. Schneider, U. Krentz, Substituted dicyanopyridines as adenosine receptor stimulators and their preparation and use for the treatment of cardiovascular diseases, 2012, WO 20122000945 A1.

[39] L.W. Jones, L.F. Werner, Aliphatic hydroxylammonium salts and hydroxamic acids with halogen substituents, J. Am. Chem. Soc. 39 (1917) 413-422.

[40] M.A.M. Gad-Elkareem, M.A.A. Elneairy, A.M. Taha, Reactions with 3,6-diaminothieno[2,3-b]-pyridines: Synthesis and characterization of several new fused pyridine heterocycles, Heteroatom Chem. 18 (2007) 405-413.

[41] D. Thimm, A.C. Schiedel, F.F. Sherbiny, S. Hinz, K. Hochheiser, D.C.G. Bertarelli, A. Maass, C.E. Müller, Ligand-Specific Binding and Activation of the Human Adenosine A_{2B} Receptor, Biochemistry 52 (2013) 726-740.

[42] D. Dal Ben, M. Buccioni, C. Lambertucci, A. Thomas, R. Volpini, Simulation and comparative analysis of binding modes of nucleoside and non-nucleoside agonists at the A_{2B} adenosine receptor, In Silico Pharmacol. 1 (2013) 24.

[43] S. Costanzi, A.A. Ivanov, I.G. Tikhonova, K.A. Jacobson, Structure and Function of G Protein-Coupled Receptors Studied Using Sequence Analysis, Molecular Modeling and Receptor Engineering: Adenosine Receptors, Front. Drug Des. Discov. 3 (2007) 63-79.

[44] D. Dal Ben, C. Lambertucci, G. Marucci, R. Volpini, G. Cristalli, Adenosine Receptor Modeling: What does the A_{2A} Crystal Structure Tell Us?, Curr. Top. Med. Chem. 10 (2010) 993-1018.

[45] G. Lebon, T. Warne, P.C. Edwards, K. Bennett, C.J. Langmead, A.G. Leslie, C.G. Tate, Agonist-bound adenosine A_{2A} receptor structures reveal common features of GPCR activation, Nature 474 (2011) 521-525.

[46] F. Xu, H. Wu, V. Katritch, G.W. Han, K.A. Jacobson, Z.G. Gao, V. Cherezov, R.C. Stevens, Structure of an agonist-bound human A_{2A} adenosine receptor, Science 332 (2011) 322-327.

[47] I. Molecular Operating Environment; C.C.G., 1255 University St., Suite 1600, Montreal, Quebec, Canada, H3B 3X3.

[48] J.J. Stewart, MOPAC: a semiempirical molecular orbital program, J. Comput. Aided Mol. Des. 4 (1990) 1-105.

[49] G. Jones, P. Willett, R.C. Glen, A.R. Leach, R. Taylor, Development and validation of a genetic algorithm for flexible docking, J. Mol. Biol. 267 (1997) 727-748.

[50] R. Huey, G.M. Morris, A.J. Olson, D.S. Goodsell, A semiempirical free energy force field with charge-based desolvation, J. Comput. Chem. 28 (2007) 1145-1152.

[51] G.M. Morris, R. Huey, W. Lindstrom, M.F. Sanner, R.K. Belew, D.S. Goodsell, A.J. Olson, AutoDock4 and AutoDockTools4: Automated docking with selective receptor flexibility, J. Comput. Chem. 30 (2009) 2785-2791.

[52] D. Dal Ben, M. Buccioni, C. Lambertucci, G. Marucci, C. Santinelli, A. Spinaci, A. Thomas, R. Volpini, Simulation and Comparative Analysis of Different Binding Modes of Non-nucleoside Agonists at the A_{2A} Adenosine Receptor, Mol. Inform. 35 (2016) 403-413.

[53] D. Rodriguez, Z.G. Gao, S.M. Moss, K.A. Jacobson, J. Carlsson, Molecular docking screening using agonist-bound GPCR structures: probing the A_{2A} adenosine receptor, J. Chem. Inf. Model. 55 (2015) 550-563.

[54] F. Vincenzi, M. Targa, R. Romagnoli, S. Merighi, S. Gessi, P.G. Baraldi, P.A. Borea, K. Varani, TRR469, a potent A_1 adenosine receptor allosteric modulator, exhibits anti-nociceptive properties in acute and neuropathic pain models in mice, Neuropharmacology 81 (2014) 6-14.

[55] K. Varani, A. Massara, F. Vincenzi, A. Tosi, M. Padovan, F. Trotta, P.A. Borea, Normalization of A_{2A} and A_3 adenosine receptor up-regulation in rheumatoid arthritis patients by treatment with anti-tumor necrosis factor alpha but not methotrexate, Arthritis Rheum. 60 (2009) 2880-2891.

[56] K. Varani, S. Merighi, S. Gessi, K.-N. Klotz, E. Leung, P.G. Baraldi, B. Cacciari, R. Romagnoli, G. Spalluto, P.A. Borea, [^{3}H]MRE 3008F20: a novel antagonist radioligand for the pharmacological and biochemical characterization of human A_3 adenosine receptors, Mol. Pharmacol. 57 (2000) 968-975.

[57] A. Ravani, F. Vincenzi, A. Bortoluzzi, M. Padovan, S. Pasquini, S. Gessi, S. Merighi, P.A. Borea, M. Govoni, K. Varani, Role and Function of A_{2A} and A_3 Adenosine Receptors in Patients

with Ankylosing Spondylitis, Psoriatic Arthritis and Rheumatoid Arthritis, Int. J. Mol. Sci. 18 (2017) 697.

[58] W.D. Cornell, P. Cieplak, C.I. Bayly, I.R. Gould, K.M. Merz, D.M. Ferguson, D.C. Spellmeyer, T. Fox, J.W. Caldwell, P.A. Kollman, A Second Generation Force Field for the Simulation of Proteins, Nucleic Acids, and Organic Molecules, J. Am. Chem. Soc. 117 (1995) 5179-5197.

[59] S. Dallakyan, A.J. Olson, Small-molecule library screening by docking with PyRx, Methods Mol. Biol. 1263 (2015) 243-250.

Graphical abstract

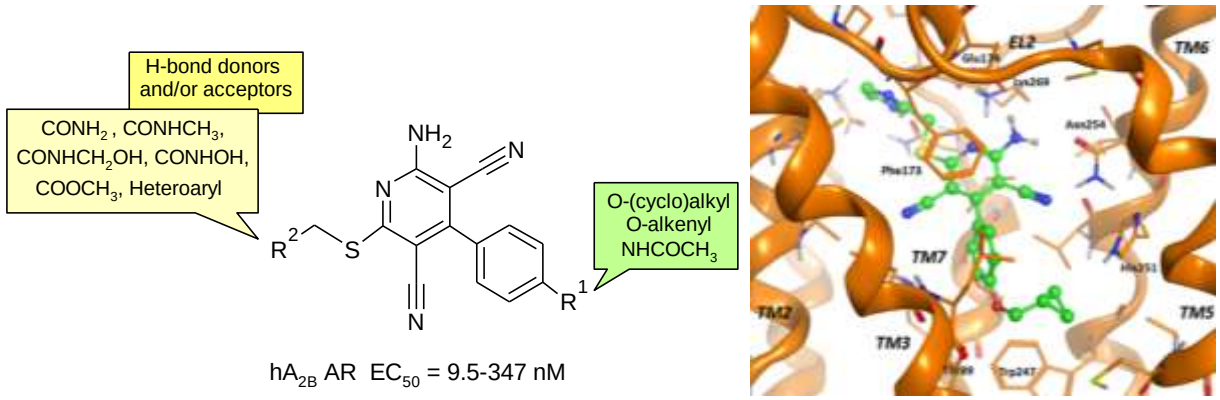

Supplementary Material

The aminopyridine-3,5-dicarbonitrile core for the design of new non-nucleoside-like agonists of the human adenosine A_{2B} receptor

Marco Betti,[a] Daniela Catarzi,[a*] Flavia Varano,[a] Matteo Falsini,[a] Katia Varani,[b] Fabrizio Vincenzi,[b] Diego Dal Ben,[c] Catia Lambertucci,[c] Vittoria Colotta[a]

[a]Dipartimento di Neuroscienze, Psicologia, Area del Farmaco e Salute del Bambino, Sezione di Farmaceutica e Nutraceutica, Università degli Studi di Firenze, Via Ugo Schiff, 6, 50019 Sesto Fiorentino, Italy; [b]Dipartimento di Scienze Mediche, Sezione di Farmacologia, Università degli Studi di Ferrara, Via Fossato di Mortara 17-19, 44121 Ferrara, Italy; [c]Scuola di Scienze del Farmaco e dei Prodotti della Salute, Università degli Studi di Camerino, Via S. Agostino 1, 62032 Camerino (MC), Italy.

Contents: Page

Table S1. Combustion Analysis data of the newly synthesized compounds

compd	Formula	C	H	N
		calcd-found	calcd-found	calcd-found
3	$C_{20}H_{19}N_5O_2S$	61.05-61.16	4.87-4.78	17.81-17.63
4	$C_{19}H_{19}N_5O_2S$	59.82-59.99	5.02-4.90	18.37-18.21

5	$C_{17}H_{15}N_5O_2S$	57.77-57.49	4.28-4.10	19.83-19.98
6	$C_{18}H_{15}N_5O_2S$	59.16-59.32	4.14-4.00	19.18-18.97
7	$C_{19}H_{17}N_5O_2S$	60.14-60.36	4.52-4.39	18.47-18.23
8	$C_{17}H_{14}N_6O_2S$	55.72-55.58	3.85-3.97	22.95-23.09
9	$C_{20}H_{19}N_5O_2S$	61.05-61.37	4.87-4.68	17.81-17.65
10	$C_{20}H_{19}N_5O_3S$	58.66-58.41	4.68-4.52	17.11-17.40
11	$C_{19}H_{17}N_5O_3S$	57.71-57.92	4.34-4.50	17.72-17.49
12	$C_{20}H_{18}N_4O_3S$	60.90-61.28	4.60-4.71	14.21-13.93
13	$C_{25}H_{21}N_5O_2S$	65.91-65.65	4.65-4.43	15.38-15.64
14	$C_{26}H_{22}N_4O_3S$	66.36-66.21	4.72-4.60	11.91-12.19
15	$C_{21}H_{18}N_6OS$	62.67-62.93	4.51-4.77	20.89-20.61
16	$C_{21}H_{18}N_6OS$	62.67-62.90	5.51-4.66	20.89-20.57
17	$C_{21}H_{20}N_6OS$	62.35-62.55	4.99-5.15	20.79-20.51
18	$C_{25}H_{20}N_6OS$	66.35-66.11	4.46-4.59	18.58-18.81
19	$C_{21}H_{18}N_6OS$	62.67-62.92	4.51-4.37	20.89-20.53
20	$C_{20}H_{17}N_7OS$	59.54-59.78	4.25-4.02	24.32-24.08
21	$C_{19}H_{16}N_8OS$	56.42-56.12	3.99-4.22	27.72-28.00
22	$C_{21}H_{18}N_6OS_2$	58.05-58.33	4.18-3.99	19.35-19.11
23	$C_{20}H_{17}N_7OS$	59.54-59.77	4.25-4.38	24.32-24.03
24	$C_{23}H_{19}N_5OS$	66.81-66.55	4.64-4.51	16.95-17.18
25	$C_{18}H_{17}N_5O_2S$	58.84-58.99	4.67-4.43	19.07-18.81
26	$C_{19}H_{16}N_6OS$	60.62-60.41	4.29-4.50	22.34-22.04
27	$C_{19}H_{16}N_6OS$	60.62-60.92	4.29-4.44	22.34-22.07
28	$C_{20}H_{16}N_6OS$	61.84-61.62	4.15-3.98	21.65-21.47

36	$C_{12}H_9N_3O$	68.22-67.98	4.30-4.15	19.90-20.21
37	$C_{24}H_{20}N_4OS$	69.88-69.55	4.89-4.71	13.59-13.83
38	$C_{23}H_{20}N_4OS$	68.98-69.32	5.04-5.21	14.00-14.29
39	$C_{21}H_{16}N_4OS$	67.72-67.48	4.33-4.11	15.05-15.37
40	$C_{22}H_{16}N_4OS$	68.73-68.98	4.20-4.37	14.58-14.30
41	$C_{23}H_{18}N_4OS$	69.33-69.58	4.56-4.24	14.07-14.32
42	$C_{21}H_{15}N_5OS$	65.44-65.13	3.92-3.70	18.17-18.39
43	$C_{23}H_{18}N_4OS$	69.33-69.58	4.56-4.38	14.07-13.80
44	$C_{18}H_{16}N_4OS$	64.27-64.01	4.80-4.97	16.67-16.88
45	$C_{17}H_{16}N_4OS$	62.94-63.15	4.98-5.12	17.28-16.99
46	$C_{15}H_{12}N_4OS$	60.80-61.11	4.08-3.88	18.92-18.68
47	$C_{16}H_{12}N_4OS$	62.32-62.03	3.93-4.11	18.18-18.42
48	$C_{17}H_{14}N_4OS$	63.34-63.59	4.38-4.19	17.39-17.12
49	$C_{15}H_{11}N_5OS$	58.24-57.97	3.59-3.41	22.65-22.91
50	$C_{17}H_{14}N_4OS$	63.34-63.10	4.38-4.45	17.39-17.63
52	$C_{19}H_{17}N_5O_2S$	60.14-60.43	4.52-4.34	18.47-18.22

Comparison of the docking conformation of compound 15 at the two A_{2B} AR model binding cavity.

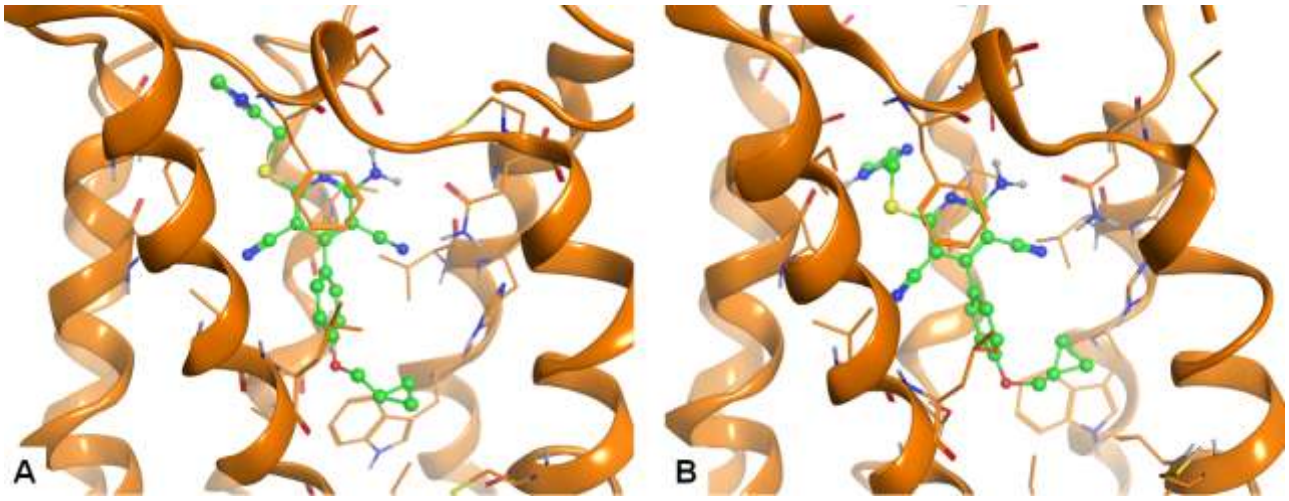

Figure S1. Compound **15** docked at the binding site of the two hA_{2B} AR receptor models; panel **A** shows the 2YDO-based receptor, while panel **B** shows the 3QAK-based one. The binding mode is highly conserved at the two cavities, as well as the interaction with the receptor residues (i.e. Asn254). The different arrangement of the residues at the entrance of the cavity (i.e. Glu174) may lead to a diverse orientation of the 2-substituent without largely modifying the compound conformation.

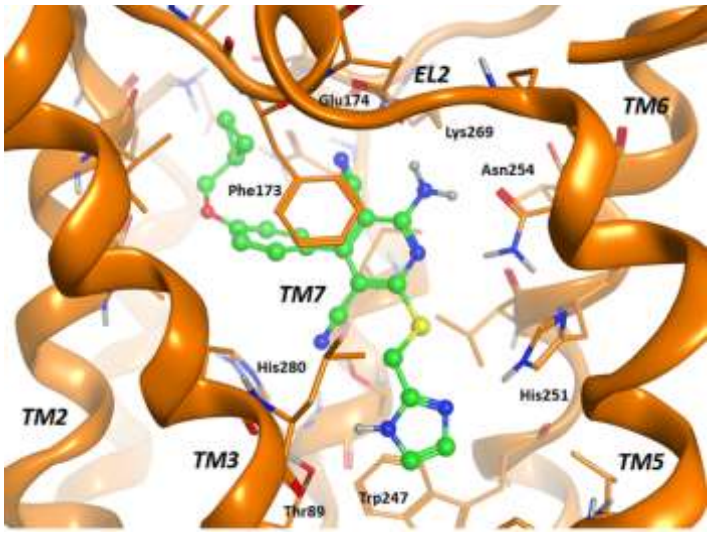

Figure S2. Alternative docking conformation of compound **15** at the hA_{2B} AR receptor model (the 2YDO-based one). Key residues for ligand-target interaction are indicated. See text below for details.

An alternative binding mode orients the compounds in a different way with respect to the docking conformations described within the main text, and similarly to the one previously described in the literature at this receptor [41,42,53]. This binding mode was associated with a good docking score only for some derivatives bearing a small R^2 substituent, in particular an amide group (**1**, **5**, **8**, **9**, **10**, **25**). In detail, the N1 atom and the 2-amino group of the pyridine core give polar interaction, respectively, with the NH and/or carbonyl groups of the Asn254$^{6.55}$ residue. The interaction between the 2-amino and the Glu174 side chain is clearly observable only in the 2YDO-based model. The 5-cyano group of pyridines gets close to His280$^{7.43}$ and Ser279$^{7.42}$. As for the general binding mode described within the main text, the interaction with these residues could be mediated by a bridge water molecule or a reorientation (or different protonation state) of His280$^{7.43}$. The 4-phenyl ring points toward residues of TM1, TM2 and TM7 and again eventual additional substituents modulate the interaction with the receptor. The 3-cyano group locates toward the extracellular environment in proximity of residues Glu174 and Lys269. The 6-sulfanyl substituent gets in proximity of TM3, TM5, and TM6 residues (Leu86$^{3.33}$, Thr89$^{3.36}$, Asn186$^{5.42}$, Trp247$^{6.48}$, and His251$^{6.52}$). In this arrangement, the amide group in R^2 appears to mimic the analogue function of adenosine-like derivatives as observed at several hA_{2A} AR crystal structures, i.e. by interacting with Thr89$^{3.36}$ and His251$^{6.52}$ (Thr88$^{3.36}$ and His250$^{6.52}$ in the hA_{2A} AR, respectively) [42,52].

^{1}H NMR and ^{13}C APT NMR spectra of representative derivatives.

The ^{13}C APT (Attached Proton Test) experiment distinguishes between C-H multiplicities. CH and CH_3 vectors have opposite phases compared to C and CH_2. Therefore, the phase of CH and CH_3 peaks is 180° different from C (including the solvent DMSO) and CH_2 peaks.

^{1}H NMR spectrum (400 MHz, DMSO-d_6) of compound **3.**

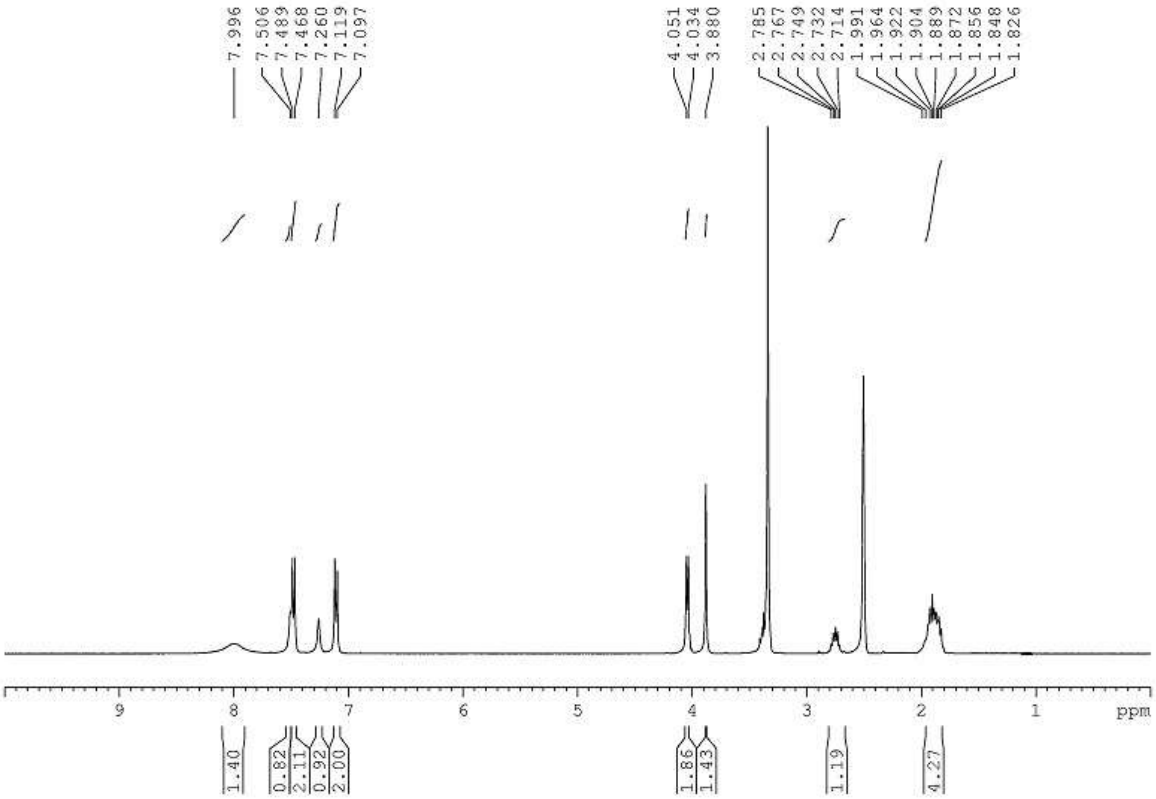
7.996
7.506
7.489
7.468
7.260
7.119
7.097
4.051
4.034
3.880
2.785
2.767
2.749
2.732
2.714
1.991
1.964
1.922
1.904
1.889
1.872
1.856
1.848
1.826
9
8
7
6
5
4
3
2
1
ppm
1.40
0.82
2.11
0.92
2.00
1.86
1.43
1.19
4.27

^{1}H NMR spectrum (400 MHz, DMSO-d_6) of compound **8.**

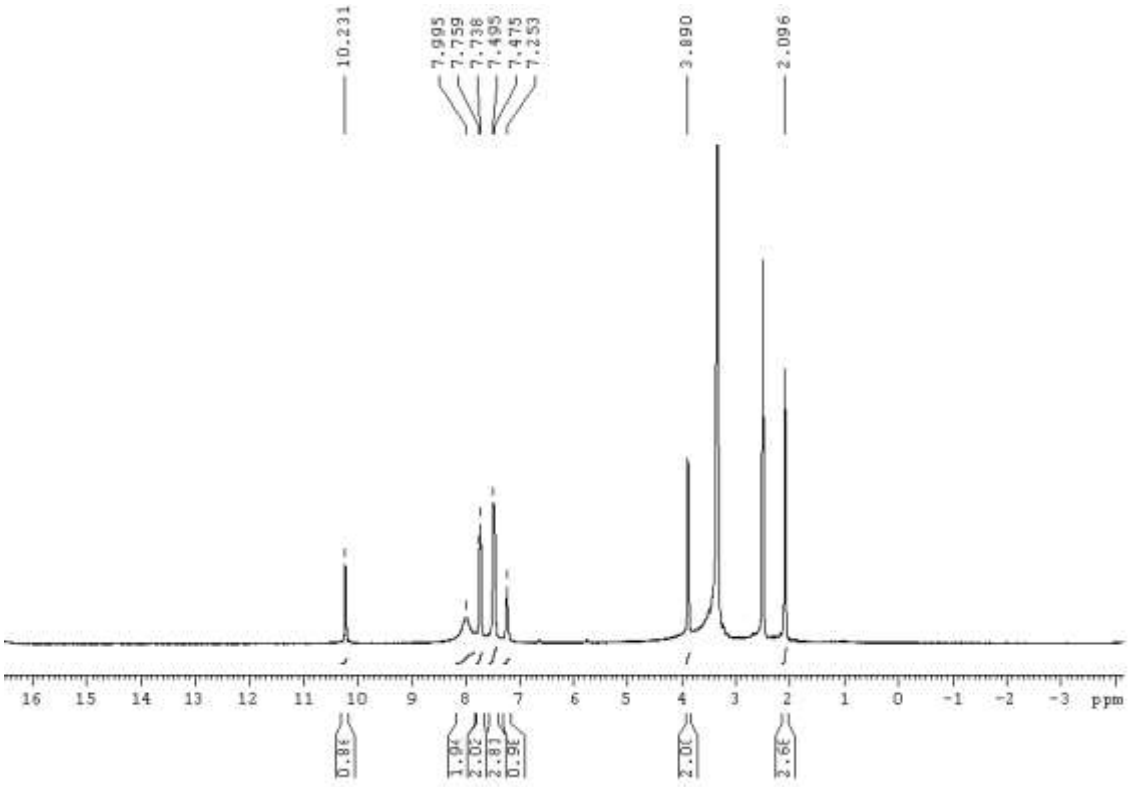

^{13}C APT NMR spectrum (100 MHz, DMSO-d_6) of compound **8**.

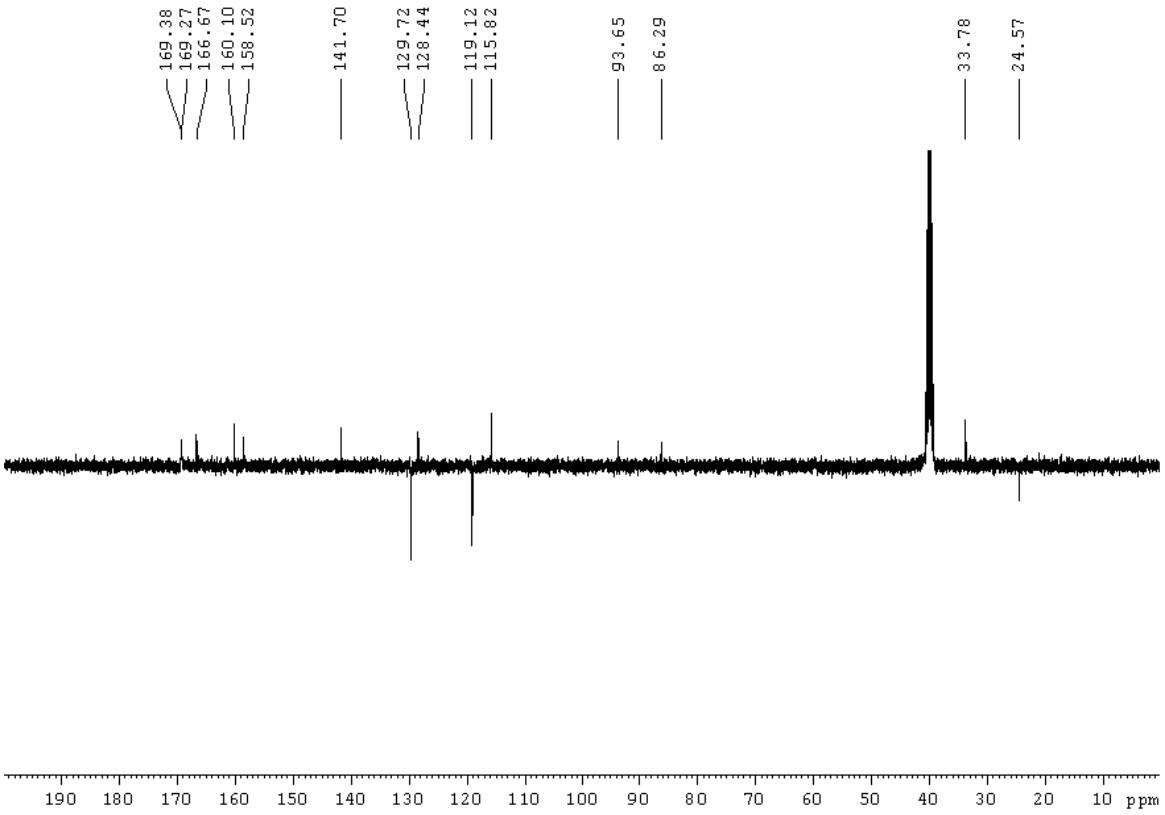

^{1}H NMR spectrum (400 MHz, DMSO-d_6) of compound **9.**

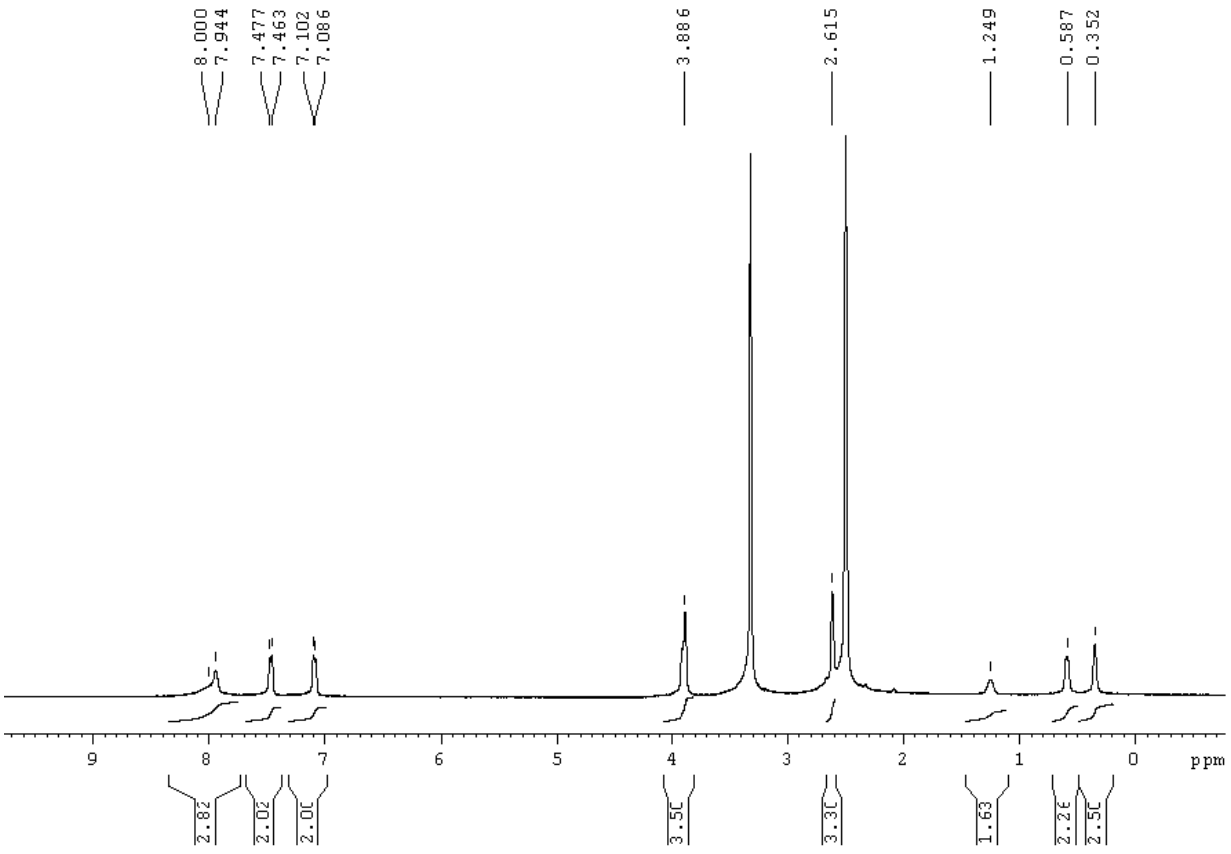

^{13}C APT NMR spectrum (100 MHz, DMSO-d_6) of compound **9**.

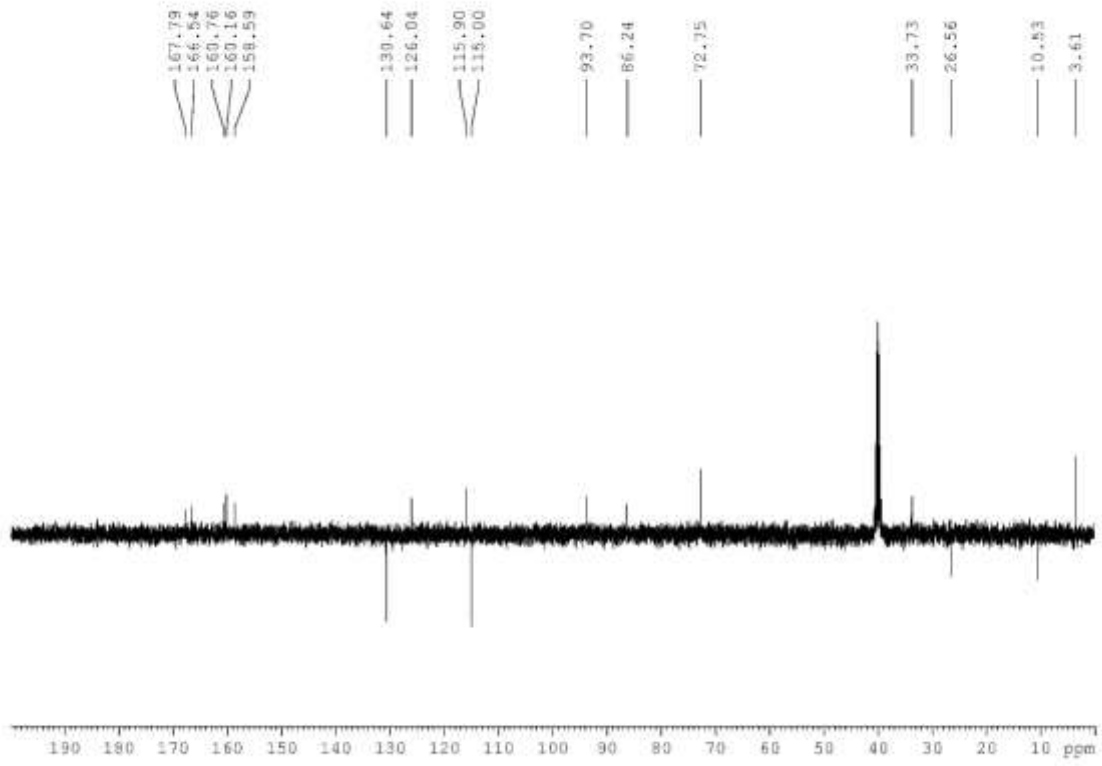

^{1}H NMR spectrum (400 MHz, DMSO-d_6) of compound **15.**

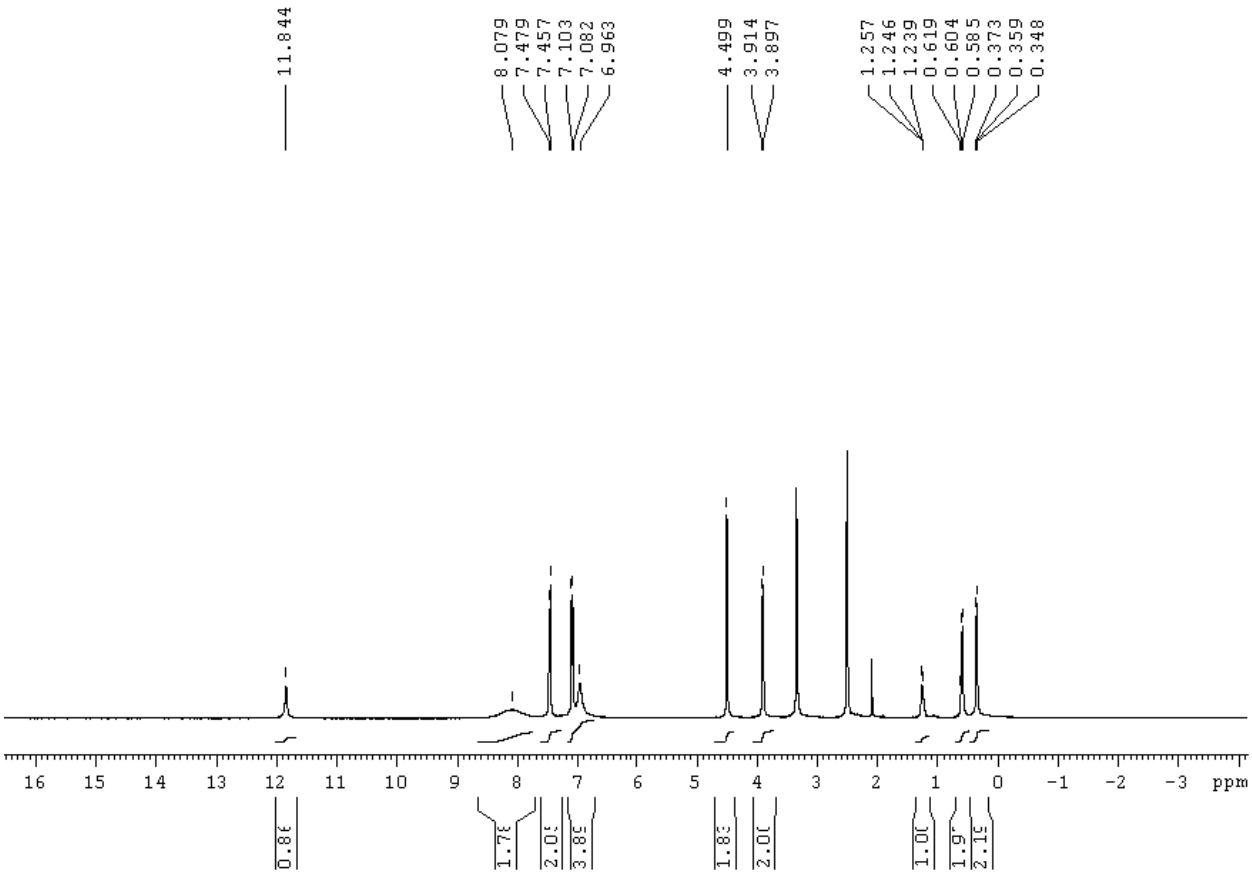

^{13}C APT NMR spectrum (100 MHz, DMSO-d_6) of compound **15**.

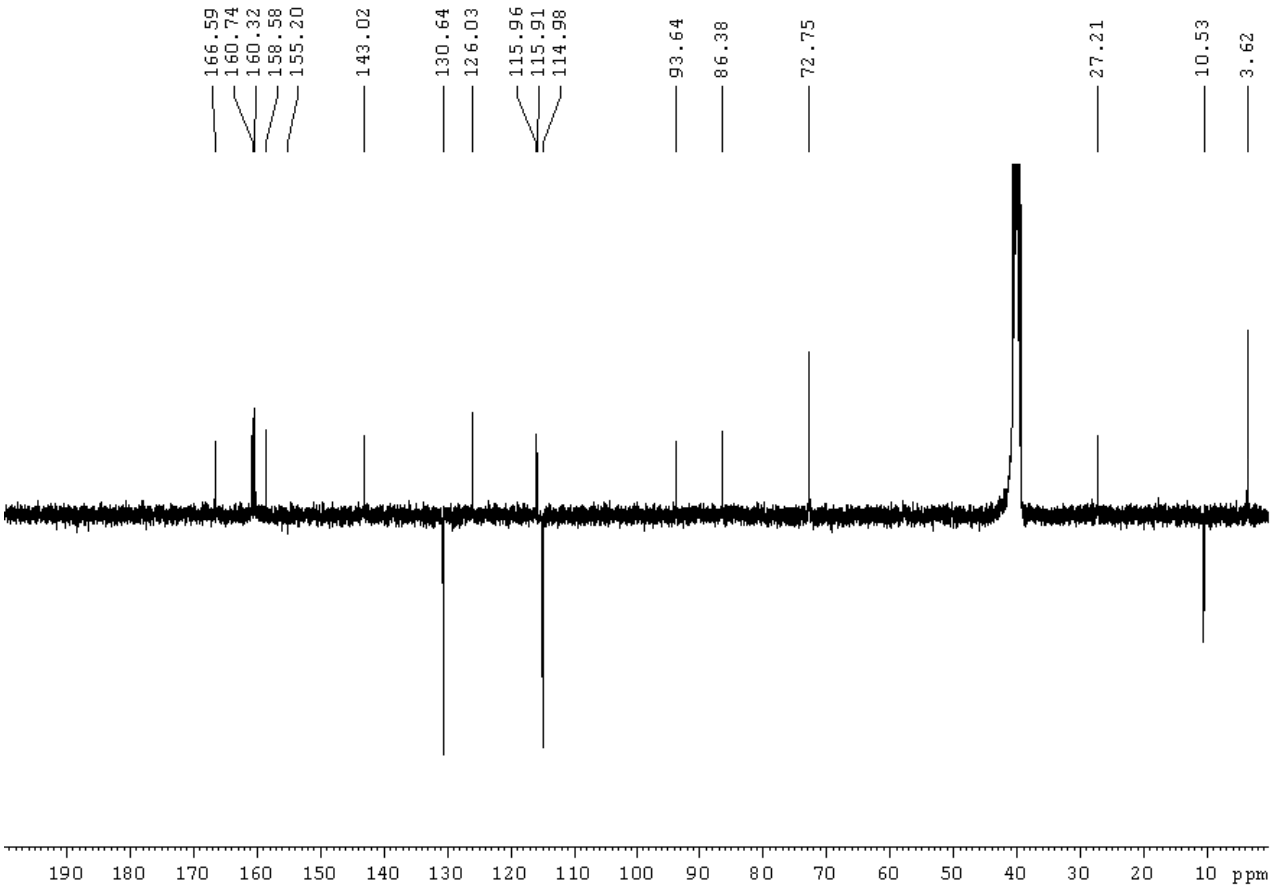

^{1}H NMR spectrum (400 MHz, DMSO-d_6) of compound **16.**

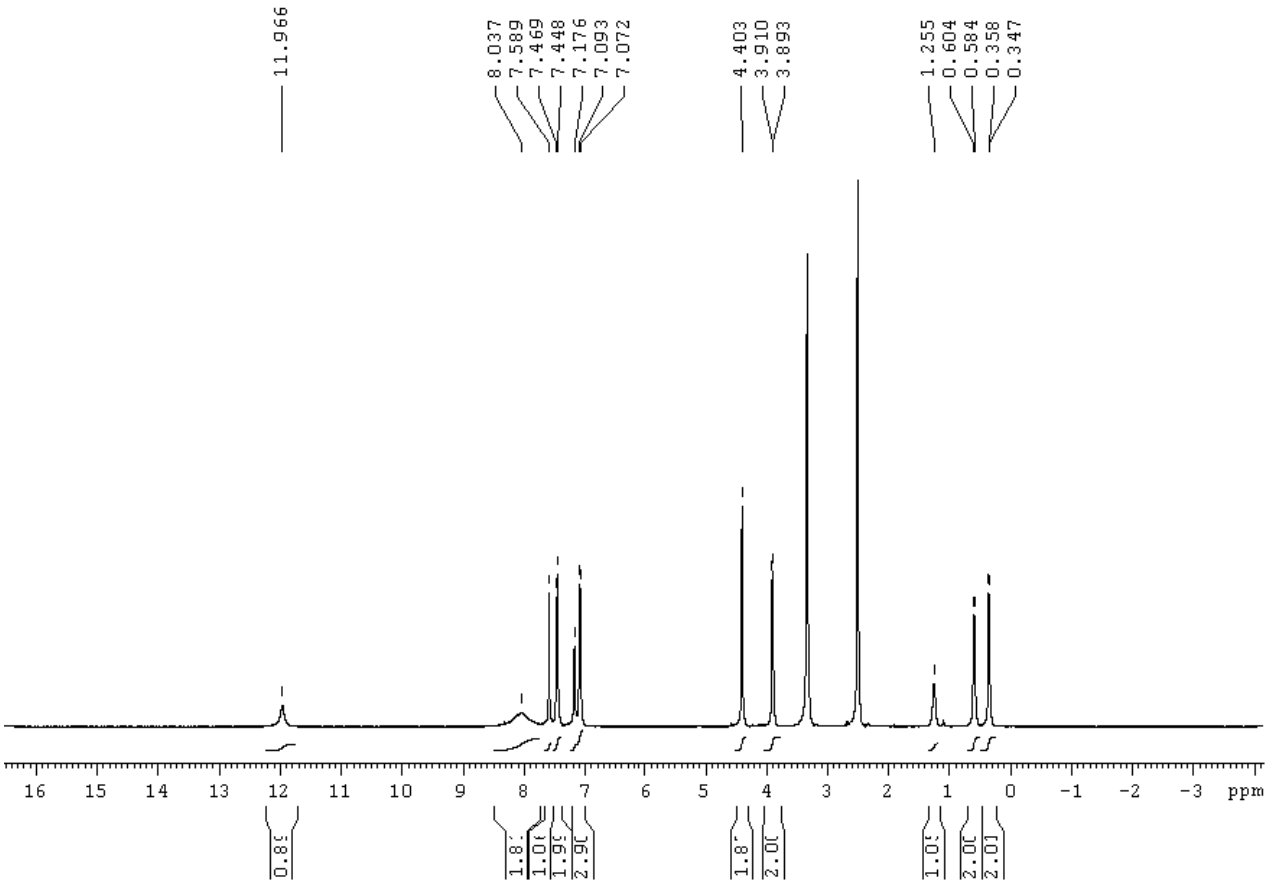

^{13}C APT NMR spectrum (100 MHz, DMSO-d_6) of compound **16**.

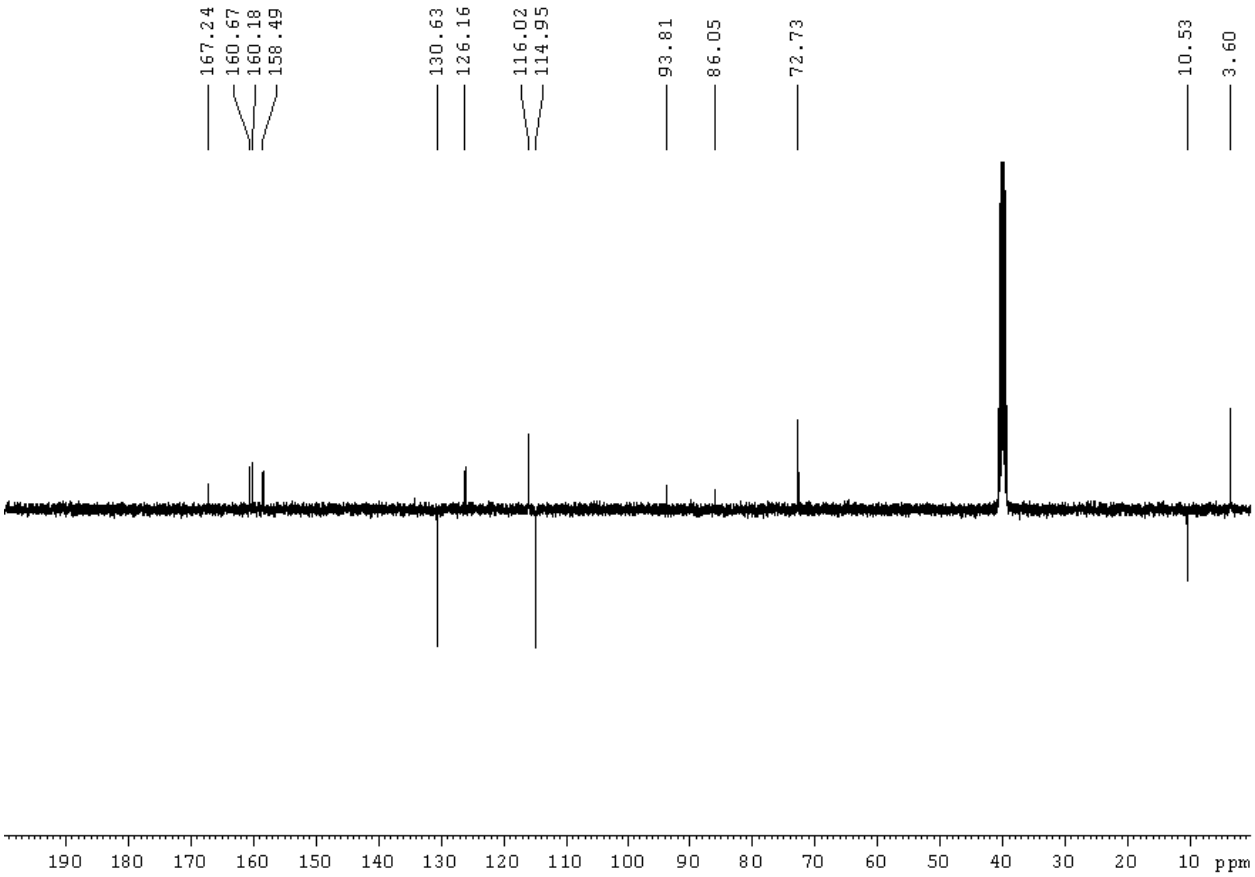

^{1}H NMR spectrum (400 MHz, DMSO-d_6) of compound **18.**

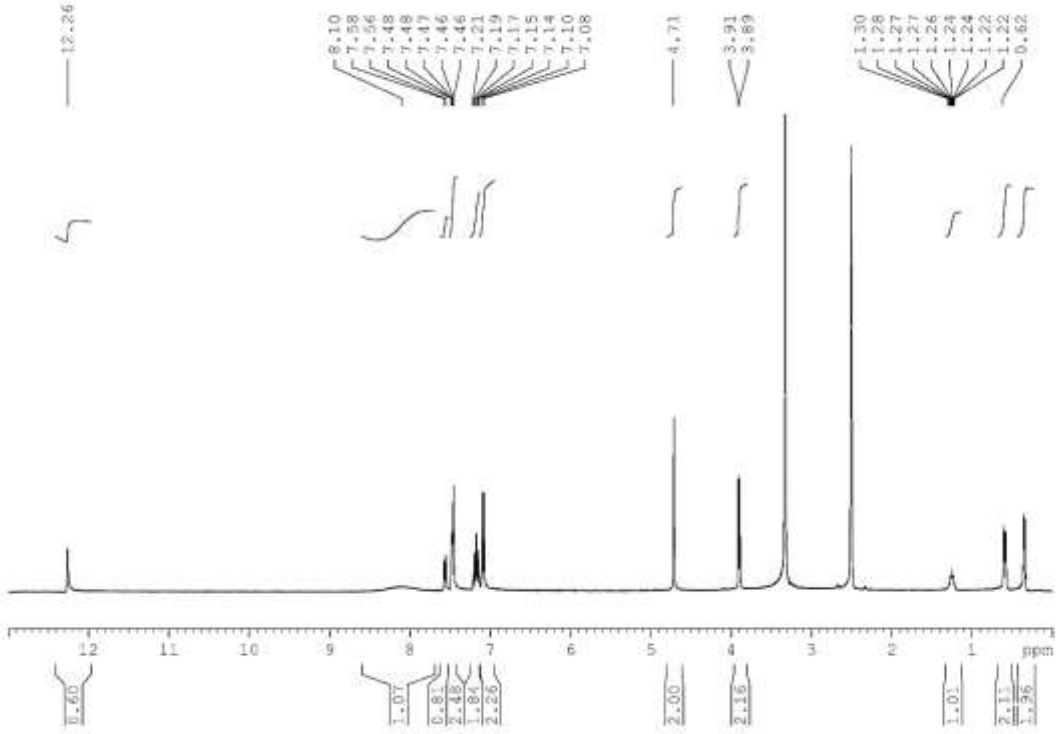
12.26
8.10
7.58
7.56
7.48
7.48
7.47
7.46
7.46
7.21
7.19
7.17
7.15
7.14
7.10
7.08
4.71
3.91
3.89
1.30
1.28
1.27
1.27
1.26
1.24
1.24
1.22
1.22
0.62
12
11
10
9
8
7
6
5
4
3
2
1
ppm
0.60
1.07
0.81
2.48
1.84
2.26
2.00
2.16
1.01
2.11
1.96
1.26

^{1}H NMR spectrum (400 MHz, DMSO-d_6) of compound **25.**

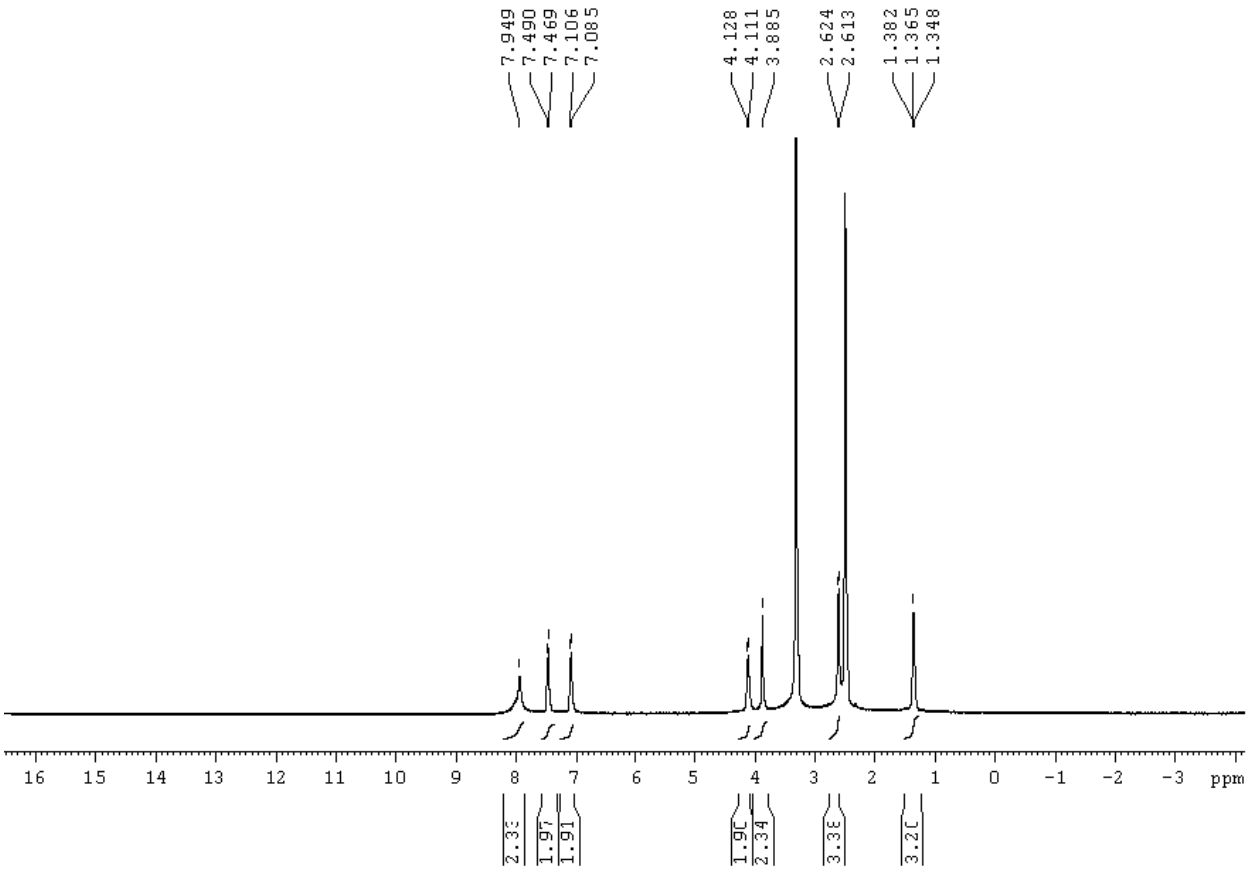

^{13}C APT NMR spectrum (100 MHz, DMSO-d_6) of compound **25**.

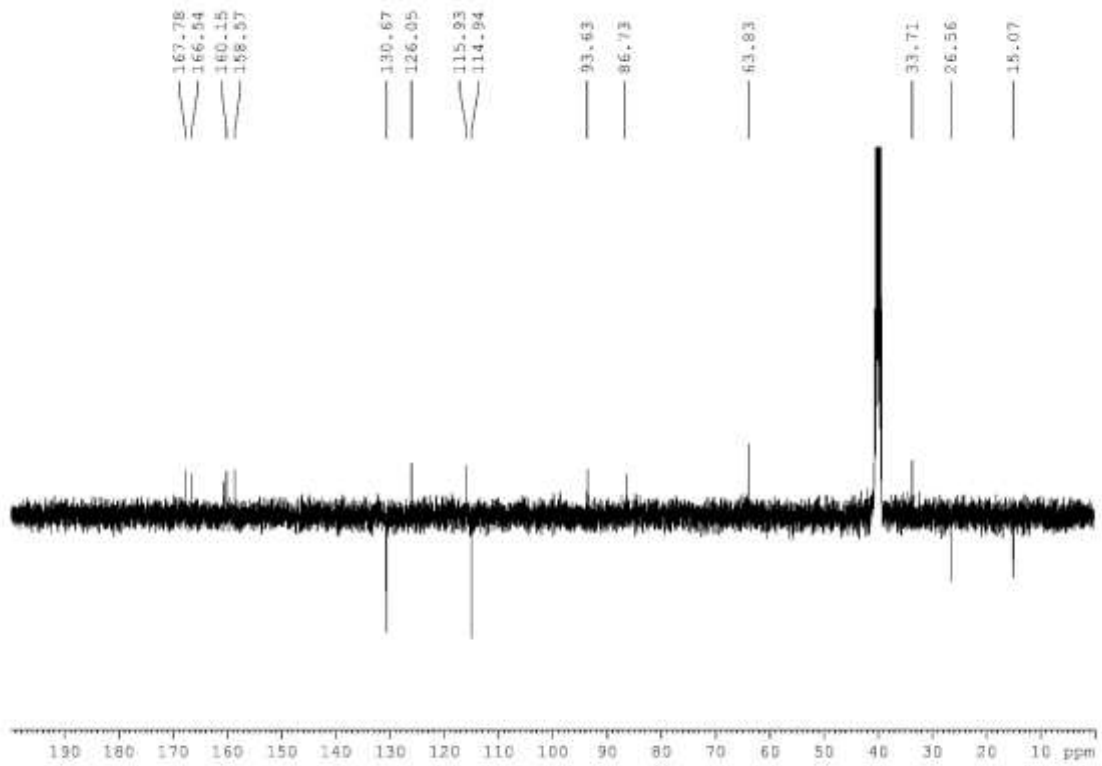

^{1}H NMR spectrum (400 MHz, DMSO-d_6) of compound **26.**

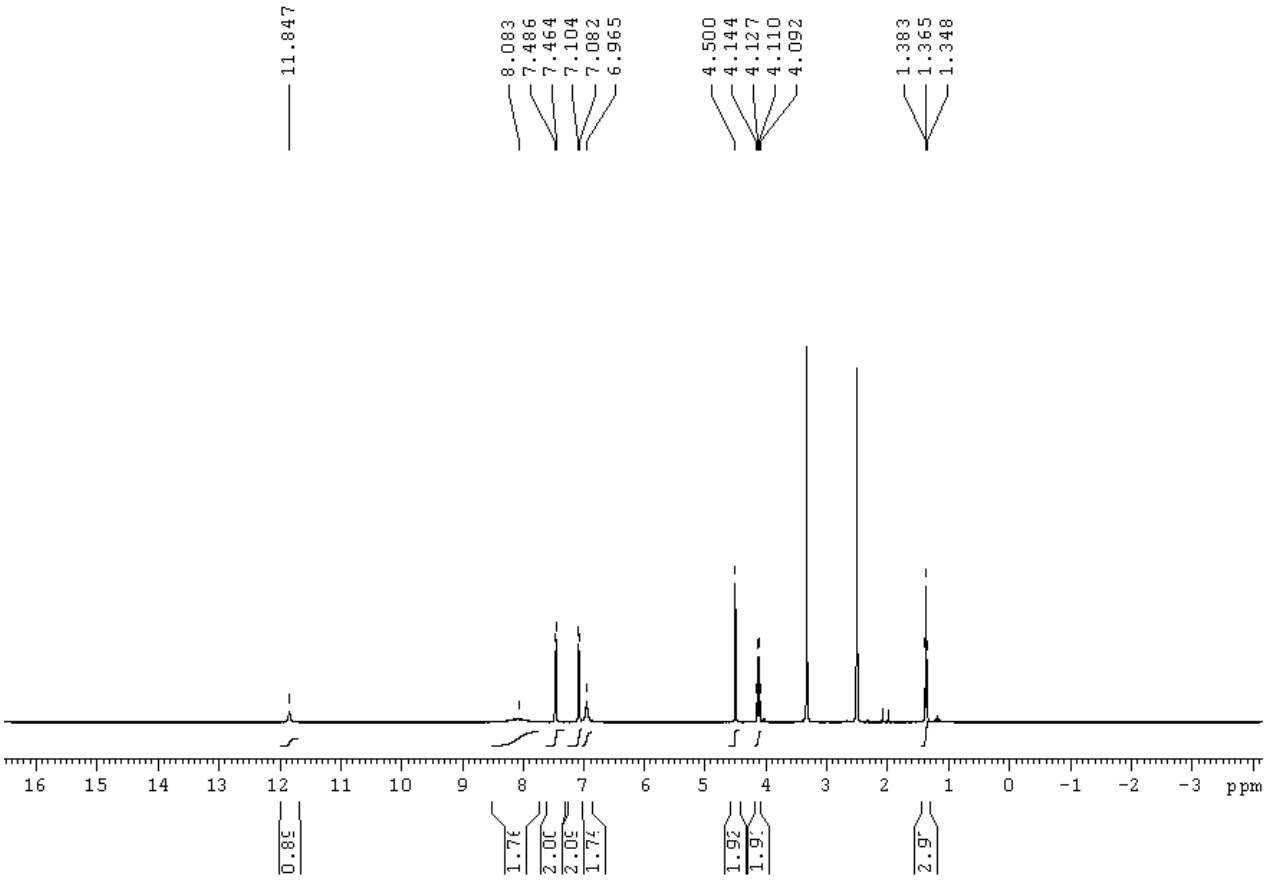

^{13}C APT NMR spectrum (100 MHz, DMSO-d_6) of compound **26**.

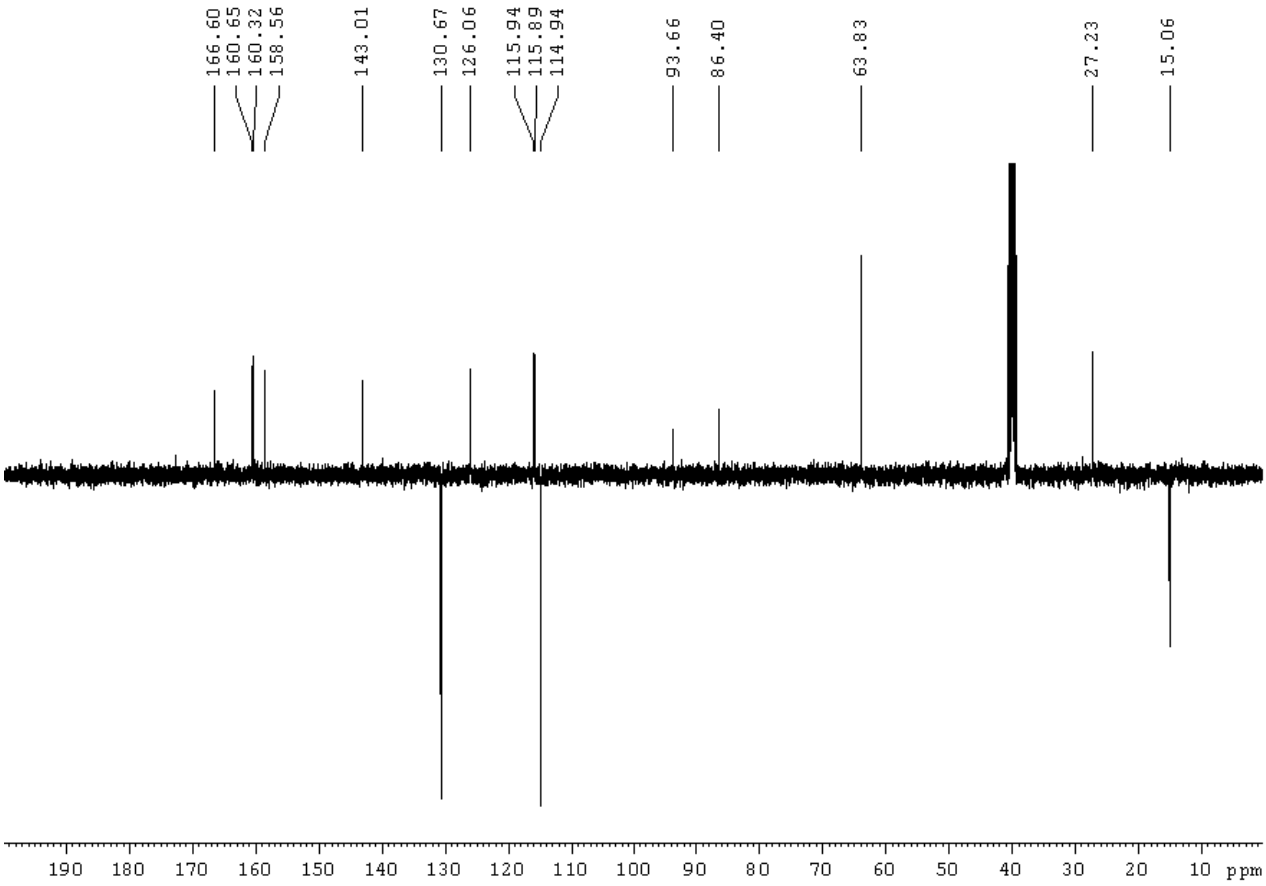

^{1}H NMR spectrum (400 MHz, DMSO-d_6) of compound **27.**

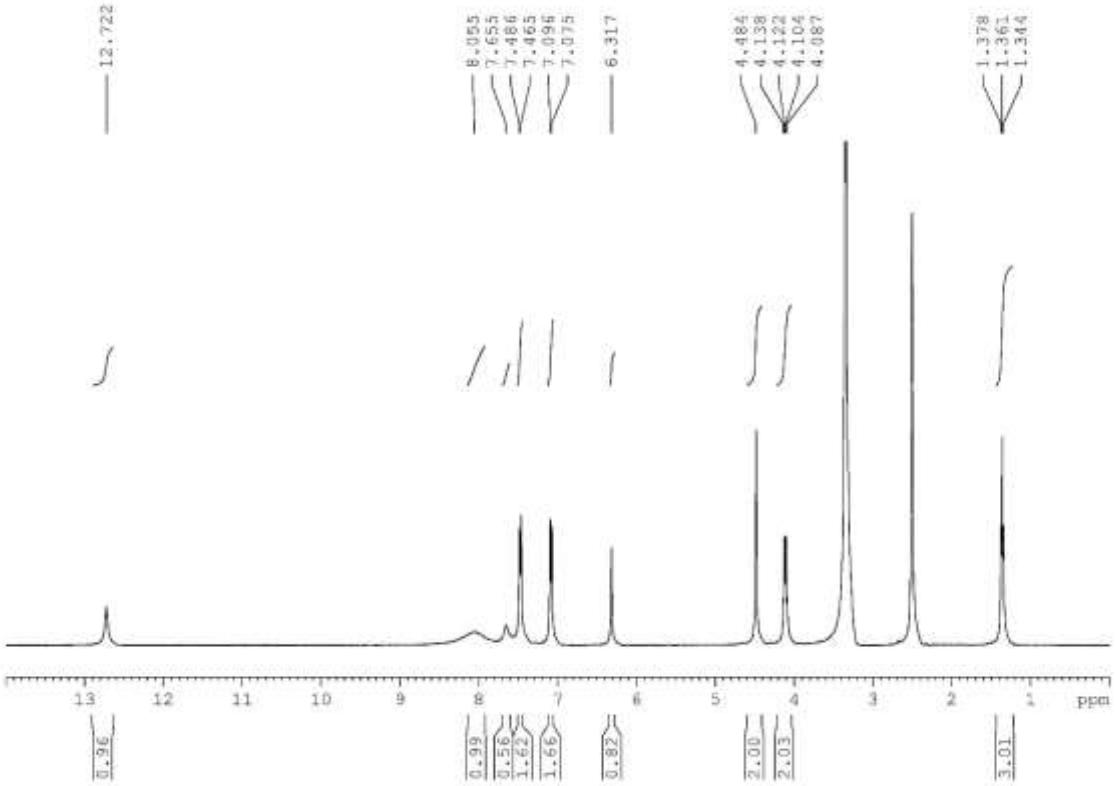
12.722
8.055
7.655
7.486
7.465
7.096
7.075
6.317
4.484
4.138
4.122
4.104
4.087
1.378
1.361
1.344
13
12
11
10
9
8
7
6
5
4
3
2
1
ppm
0.96
0.99
0.56
1.62
1.66
0.82
2.00
2.03
3.01

^{1}H NMR spectrum (400 MHz, DMSO-d_6) of compound **28.**

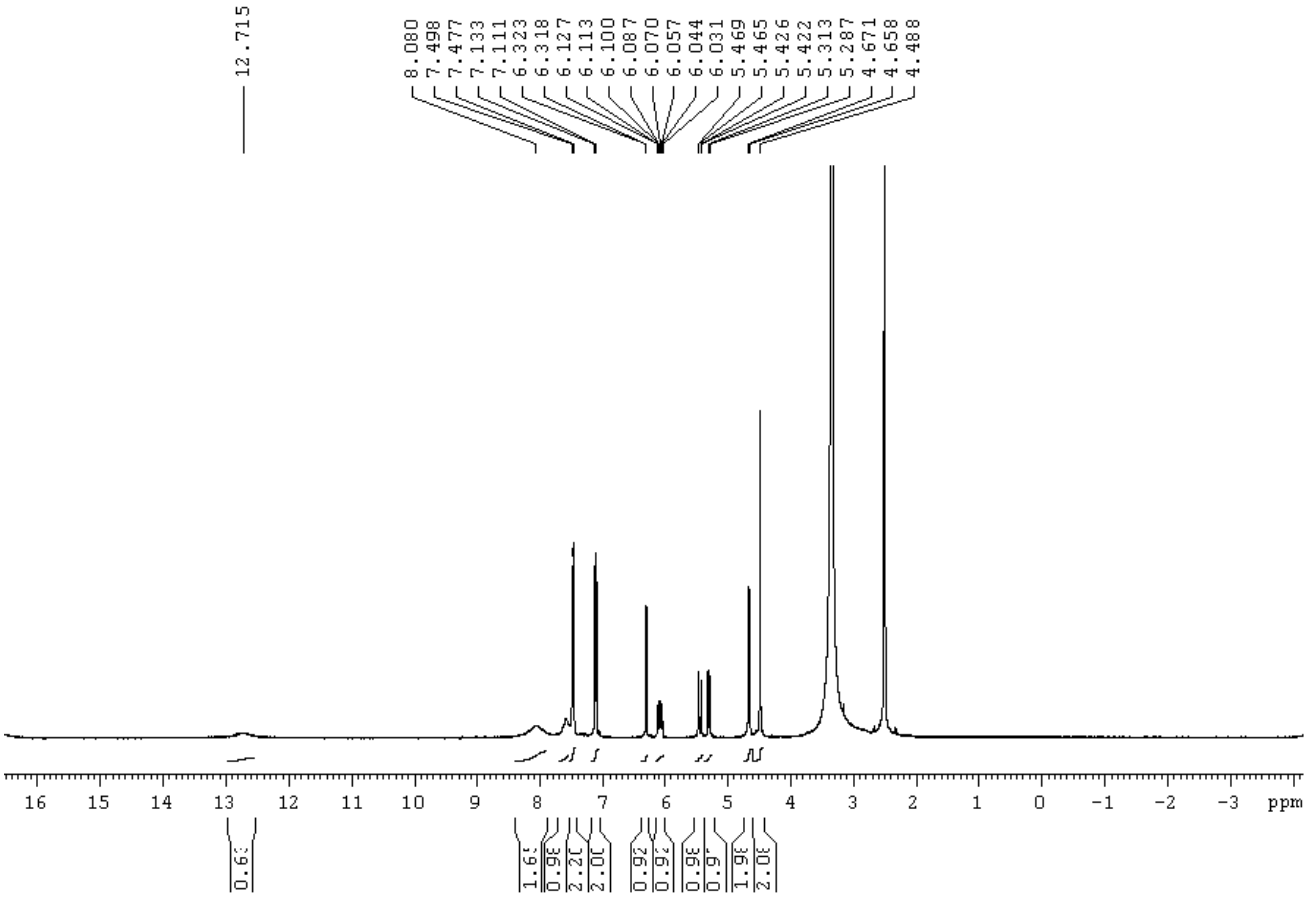

^{13}C APT NMR spectrum (100 MHz, DMSO-d_6) of compound **28**.

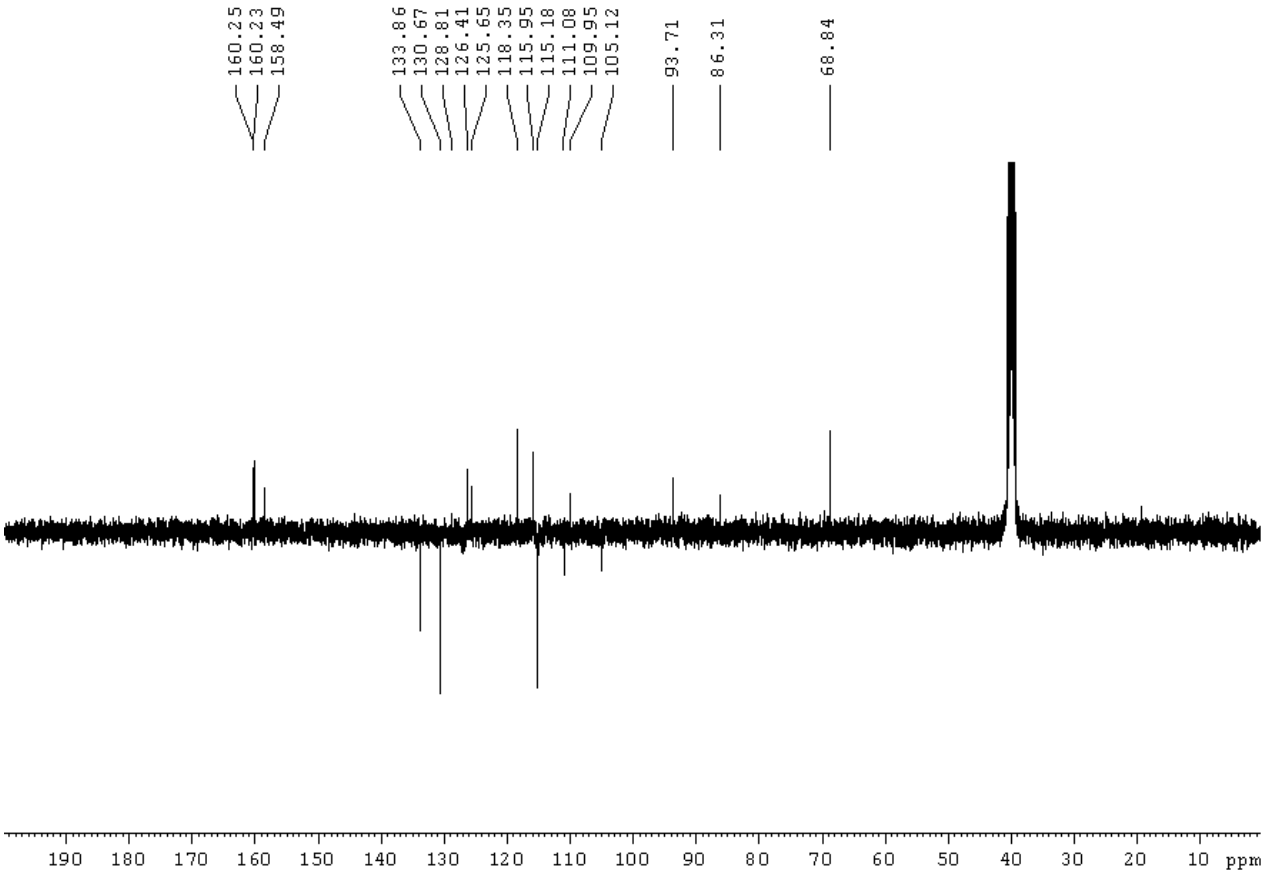

^{1}H NMR spectrum (400 MHz, DMSO-d_6) of compound **52.**

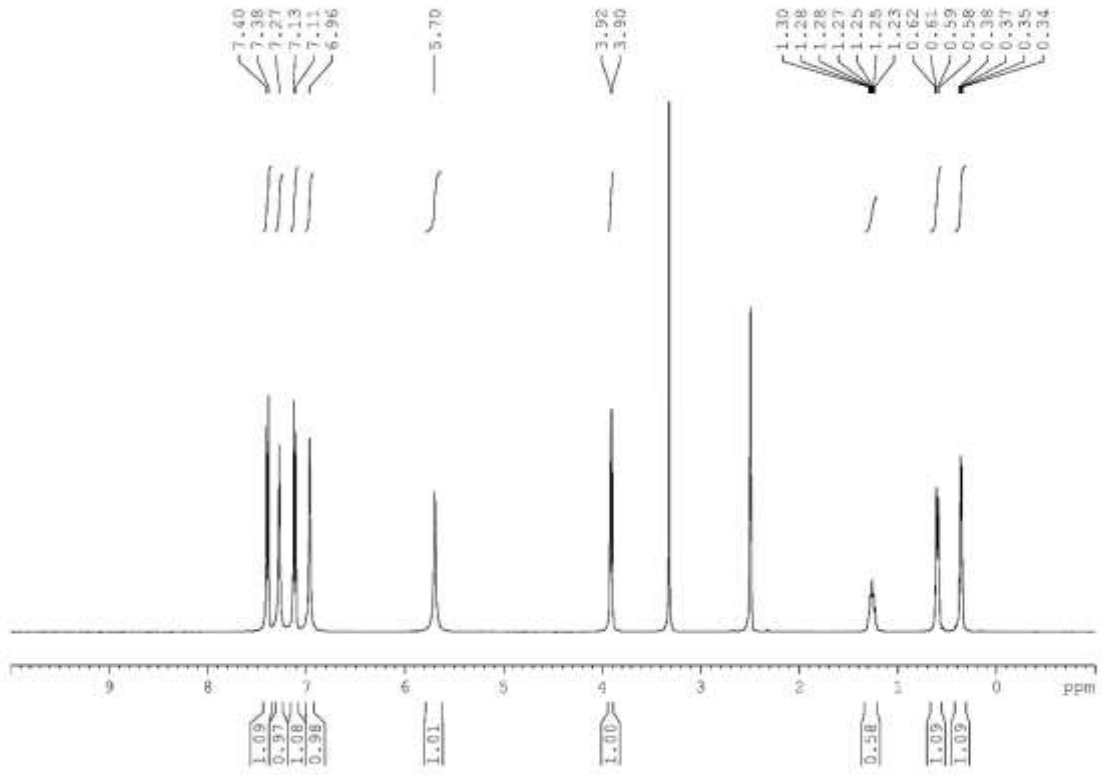

^{13}C APT NMR spectrum (100 MHz, DMSO-d_6) of compound **52**.